Atrial Abnormalities and Atrial Septal Defects

7

Louis I. Bezold

Abstract

Transesophageal echocardiography (TEE) allows for a comprehensive assessment of atrial chamber and interatrial septal anatomy. Due to the posterior position of the probe and its proximity to atrial structures, high resolution imaging of the atria and atrial septum represent a particular strength of this modality. Combined with color flow mapping and spectral Doppler interrogation, TEE is able to characterize communications at the atrial level, anatomic variants of the atria, and pathologic conditions that may affect these structures. This chapter focuses on the role of TEE in the characterization of atrial septal defects and atrial abnormalities such as juxtaposition of the atrial appendages and cor triatriatum.

Keywords

Transesophageal echocardiography • Atrial septal defects • Atrial communications • Patent foramen ovale • Atrial abnormalities • Juxtaposition of the atrial appendages • Cor triatriatum

Introduction

Transesophageal echocardiography (TEE) provides for a comprehensive evaluation of atrial chamber and interatrial septal anatomy in essentially all patients in whom this modality is feasible. Due to the proximity of the interrogating probe to the posterior aspect of the heart, high resolution imaging of atrial structures is a particular strength of the technology. This imaging approach, combined with Doppler assessment, is able to define atrial anatomy and details of the interatrial septum including communications at this level, as well as provide information regarding variants and pathologies that may affect these structures. This chapter addresses the role of TEE in the characterization of atrial septal defects and conditions such as juxtaposition of the atrial appendages and cor triatriatum.

L.I. Bezold, MD
Department of Pediatrics, Kentucky Children's Hospital, University of Kentucky College of Medicine, 800 Rose St., MN 150, Lexington 40536, KY, USA
e-mail: louis.bezold@uky.edu

General Comments

Transthoracic echocardiographic (TTE) evaluation of the atria, including complete evaluation of the interatrial septum for the presence of shunting, can be challenging in older children, teenagers, and adults due to limited subcostal acoustic windows. TEE overcomes this limitation while providing for optimal visualization of both atria, including the atrial appendages and venous connections [1–4]. TEE is often utilized and demonstrated to be highly useful in the operating room and/or cardiac catheterization laboratory to define atrial anatomy, presence, size, and location of septal defects, to evaluate postoperative results in related interventions, and to assist in transcatheter interventions that involve the atrial septum. Although a number of centers do not routinely use intraoperative TEE for straightforward surgical closures of secundum atrial septal defects, this imaging approach can be extremely helpful in documenting adequate cardiac de-airing prior to separation from cardiopulmonary bypass, and for facilitating overall intraoperative care.

The online version of this chapter (doi:10.1007/978-1-84800-064-3_7) contains supplementary material, which is available to authorized users.

P.C. Wong, W.C. Miller-Hance (eds.), *Transesophageal Echocardiography for Congenital Heart Disease*,
DOI 10.1007/978-1-84800-064-3_7,

Pulmonary and systemic venous connections can often be verified by TEE (Chap. 6). Evaluation for intracardiac thrombi, particularly to exclude an atrial thrombus prior to cardioversion in atrial fibrillation, or in potential "low-flow" states such as may be the case in the postoperative Fontan patient, can be more completely and accurately accomplished by TEE as compared to TTE (Chap. 16). This is particularly true in patients who have undergone previous modifications of the Fontan procedure such as direct atriopulmonary connections, which are generally seen in older patients with poor transthoracic acoustic windows.

In patients with neurologic findings suggestive of transient ischemic attacks or cerebral vascular accidents, the use of TEE, particularly in combination with agitated saline injection, increases the sensitivity in the detection of right-to-left flow through a patent foramen ovale.

The early experience regarding the applications of three-dimensional TEE in the evaluation of anomalies of the atria and atrial septum has already demonstrated unique benefits and in some cases superior morphologic assessment as compared to two-dimensional (2D) TEE (Chaps. 19 and 20) [5–10].

Atrial Septal Defects

Atrial septal defects (ASDs) are relatively common, accounting for approximately 7–8 % of congenital heart disease (CHD) [11]. These can occur in isolation, or may be associated with other congenital cardiac abnormalities. Communications that allow for interatrial shunting may be due to either morphologic defects involving the interatrial septum or in a location outside the confines of the septum as discussed below. The location of the defect generally reflects its underlying embryologic origin. The hemodynamic perturbations and clinical findings of a defect are largely related to its anatomic location and size, as modified by the presence or absence of potentially associated structural cardiac lesions and the relative pulmonary and systemic vascular resistances.

This chapter will focus on isolated defects, which are usually classified according to their location. Isolated ASDs include those involving the fossa ovalis (secundum ASD), defects either superior or inferior to the fossa ovalis and involving the connections of the vena cavae (superior or inferior sinus venosus type ASDs, for superior and inferior vena cava respectively), and coronary sinus defects. A patent foramen ovale (PFO) also represents a communication between the right and left atria. Although generally not considered a true ASD in the strictest sense because there is no true deficiency of atrial septal tissue [12], PFOs may become clinically significant in situations where an elevation in right atrial pressure causes right-to-left interatrial shunting through the foramen, thus representing a potential risk for paradoxical embolization. So-called primum ASDs (partial atrioventricular septal or canal defects) are considered under atrioventricular septal defects and they will be addressed only briefly in this chapter. These defects are discussed in depth in Chap. 8.

Secundum Atrial Septal Defect

Secundum ASDs, the most common type of ASD (~70 % of ASDs), are generally located within the area bordered by the limbus of the fossa ovalis. They generally result from a deficiency the in septum primum, of variable size and extent. These defects may constitute single communications, or so-called fenestrated defects with multiple orifices. They may be variably positioned, which can influence efforts at transcatheter closure. Fenestrated ASDs are often associated with an aneurysmal septum primum of the foramen. Care must be taken to identify the Eustachian valve of the right atrium (RA), which connects to the limbus of the fossa ovalis and may be mistaken for the lower edge of an ASD by echocardiography or at the time of surgery. If this error occurs during the echocardiographic evaluation, the size of the ASD could be overestimated. If it occurs during surgery, attachment of an ASD patch to this structure will have the unintended effect of diverting inferior vena cava flow directly into the left atrium (LA), resulting in significant cyanosis.

Secundum ASDs may occur in isolation or in association with many other congenital cardiac defects, including other types of ASDs [13–16]. Most secundum ASDs occur sporadically, however some occur in conjunction with defined syndromes (such as Holt-Oram or heart-hand syndrome) or gene defects [17–22].

Primum Atrial Septal Defect

Primum ASDs are the second most common type of ASD (~20 % of all ASDs). These defects are located in the most inferior and posterior portion of the atrial septum, involving the atrioventricular septum, and are invariably associated with a large "cleft" (or commissure) in the anterior leaflet of the mitral valve. They comprise one part of the spectrum of atrioventricular septal (endocardial cushion) defects, hence they are also called partial atrioventricular canal defects. These defects are discussed in full detail in Chap. 8.

Sinus Venosus Atrial Septal Defect

Sinus venosus ASDs (~10 % of ASDs) are characterized by a communication between the atrial chambers in juxtaposition to either the superior or inferior vena cava. Associated malposition

of the insertion of either the superior or inferior vena cava results in these structures straddling the atrial septum with the interatrial communication generally located within the orifice of the overriding caval vein. Superior sinus venosus defects (also known as superior vena caval defects) are located immediately inferior or caudal to the orifice of the superior vena cava and above the superior limbus of the fossa ovalis. This is the most common type of defect. Anomalous drainage of the right upper as well as in some cases, the right middle pulmonary vein often accompanies this type of defect [23, 24].

The less common inferior sinus venosus defects (also known as inferior vena caval defects) are located immediately superior/cranial to the orifice of the inferior vena cava (posterior and inferior to the fossa ovalis, which may demonstrate hypoplasia or anterior displacement of the posterior limbus). These defects are also associated with partial anomalous right pulmonary venous drainage [25–28].

Sinus venosus defects result from a deficiency in the wall that normally separates the LA from the respective caval veins. Since they are located outside the confines of the atrial septum, it has been suggested that they do not represent 'true' septal defects.

Coronary Sinus Atrial Septal Defect

Coronary sinus ASDs are rare (<1 % of ASDs) and result from either a partial deficiency or complete absence (unroofed coronary sinus) of the superior aspect of the common wall between the coronary sinus and the LA. Interatrial shunting occurs through the defect in the coronary sinus wall on the left atrial side, which is continuous with the coronary sinus opening on the right atrial side of the septum. There may be additional deficiency of atrial septal tissue surrounding the coronary sinus orifice on the right side. A common association is a persistent left superior vena cava draining to the coronary sinus [29]. These defects may also be seen in complex CHD in association with heterotaxy syndrome, atrial situs abnormalities, and with other anomalies of systemic venous return [30–32].

Patent Foramen Ovale

A PFO is present in approximately 15–30 % of normal adult hearts. Inter-atrial shunting can potentially occur if right atrial pressure exceeds left atrial pressure (right-to-left) or with normal atrial pressures if the flap valve (septum primum) of the foramen ovale is incompetent (left-to-right shunt). Transient increases in right atrial pressure do occur normally during early ventricular systole and with inspiration and can be induced by the Valsalva maneuver. A persistent, large Eustachian valve can also direct inferior vena caval blood preferentially towards the fossa ovalis and potentially across a PFO throughout the cardiac cycle [33]. An important issue related to a PFO is its potential association with paradoxical embolism and stroke, rare complications in children. TEE is more sensitive than transthoracic imaging for detection of PFO shunting. The injection of agitated saline via a peripheral or central venous catheter enhances the sensitivity of detecting a PFO [34, 35]. The presence of an atrial septal aneurysm in association with a PFO has been implicated in an increased risk of paradoxical emboli and neurologic events [36–40].

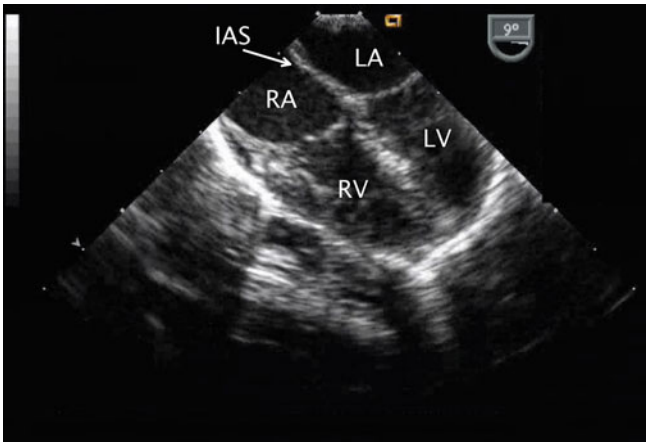

Fig. 7.1 The mid esophageal four chamber view represents a starting point in the evaluation of atrial septal defects as this cross-section displays both atria, the interatrial septum (*IAS*), atrioventricular valves, and ventricular inflows. *LA* left atrium, *LV* left ventricle, *RA* right atrium, *RV* right ventricle

Transesophageal Echocardiographic Evaluation

The interatrial septum is generally well oriented with respect to 2D imaging and Doppler interrogation with the probe at the mid esophageal four chamber (ME 4 Ch) view [41]. Probe rotation clockwise in an otherwise normal heart may enhance this view. Evaluation of the atrial septum thus begins in this view (plane ~0°–20°). This cross section demonstrates both atria and the interatrial septum (Fig. 7.1, Video 7.1). Slight probe retroflexion, if possible without losing contact with the anterior esophagus, optimizes imaging. Right and left probe shaft rotation enhances visualization of right-sided or left-sided structures respectively.

Secundum ASDs, in general, are adequately visualized in this view with slight clockwise probe shaft rotation (Fig. 7.2, Video 7.2). Color flow Doppler interrogation in this plane demonstrates the presence and direction of shunting across the interatrial septum that can be verified by pulsedwave Doppler. This assessment also assists in the characterization of the flow across an interatrial communication in terms of the presence or absence of restriction (Fig. 7.3, Video 7.3). Slight probe withdrawal may be required to visualize small superior secundum defects, or probe advancement for small inferior

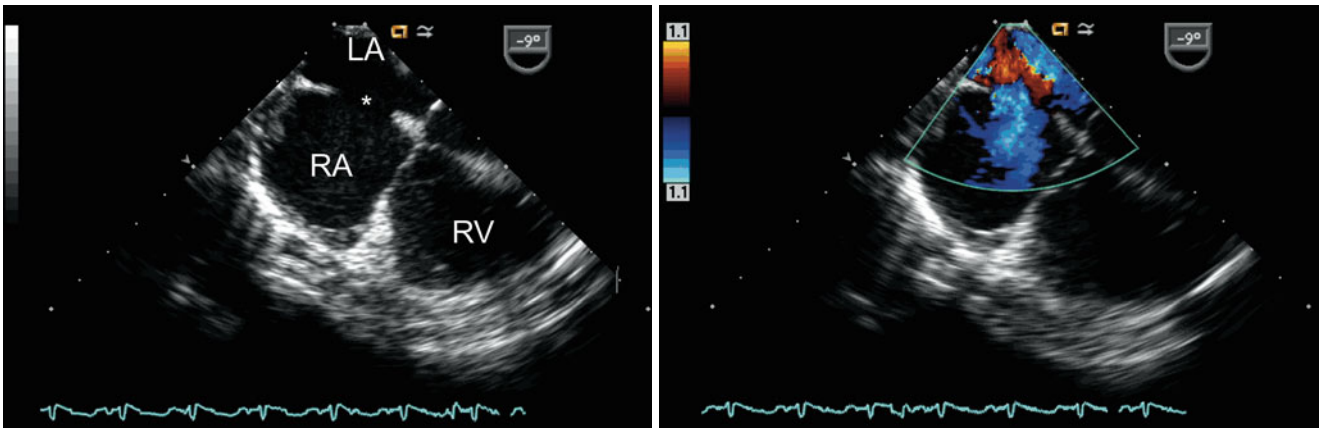

Fig. 7.2 *Left panel:* Centrally located secundum atrial septal defect (*asterisk*) shown as seen in the mid esophageal four chamber view. *Right panl:* Color flow Doppler interrogation demonstrates left-to-right shunting across the defect (*blue signal*). Note that the probe has been rotated rightwards in this view to focus on the atrial communication. *LA* left atrium, *RA* right atrium, *RV* right ventricle

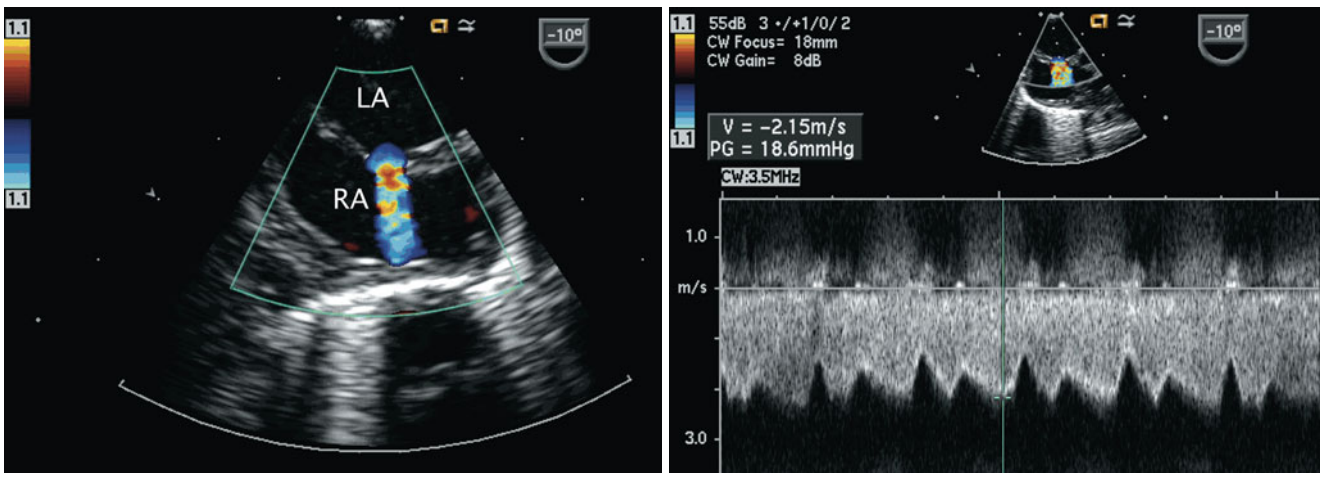

Fig. 7.3 *Left panel:* Image of the interatrial septum in the mid esophageal four chamber view with rightwards probe rotation. Note the aliased nature (mosaic of colors) of the jet across the atrial communication consistent with restriction across a small secundum atrial septal defect. The interatrial septum bulges in the rightwards direction suggesting elevated left atrial pressures. *Right panel:* Spectral Doppler interrogation confirms the restricted, high velocity flow across the defect with reduced phasic variation. *LA* left atrium, *RA* right atrium

secundum defects. Minimal probe shaft movements enhance the 2D evaluation allowing for examination of the defect in relation to adjacent structures as well as interrogation of the rims of the defect (Fig. 7.4). At times, smaller and/or more eccentric atrial defects will be detected in a standard TEE view (e.g. ME 4 Ch) *only* when a thorough sweep is performed of the septum. This emphasizes the importance of full sweeps when assessing communications at the atrial septum, as well as many other defects (Video 7.4).

Progressive withdrawal of the probe in the ME 4 Ch view to above the level of the fossa ovalis demonstrates the superior aspect of the interatrial septum—the location of superior sinus venosus defects (Fig. 7.5, Video 7.5)—as well as the superior vena cava in cross-section. Anomalous drainage of the pulmonary veins as they enter the vena cavae can be seen from these views and attempts to visualize all veins should be made. The ME 4 Ch view also allows for 2D assessment

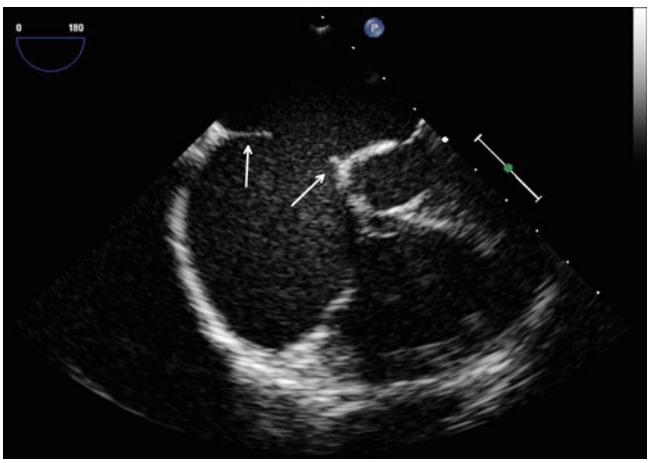

Fig. 7.4 Image displays the rims (*arrows*) of a secundum atrial septal defect in the mid esophageal four chamber view with slight rightwards probe rotation

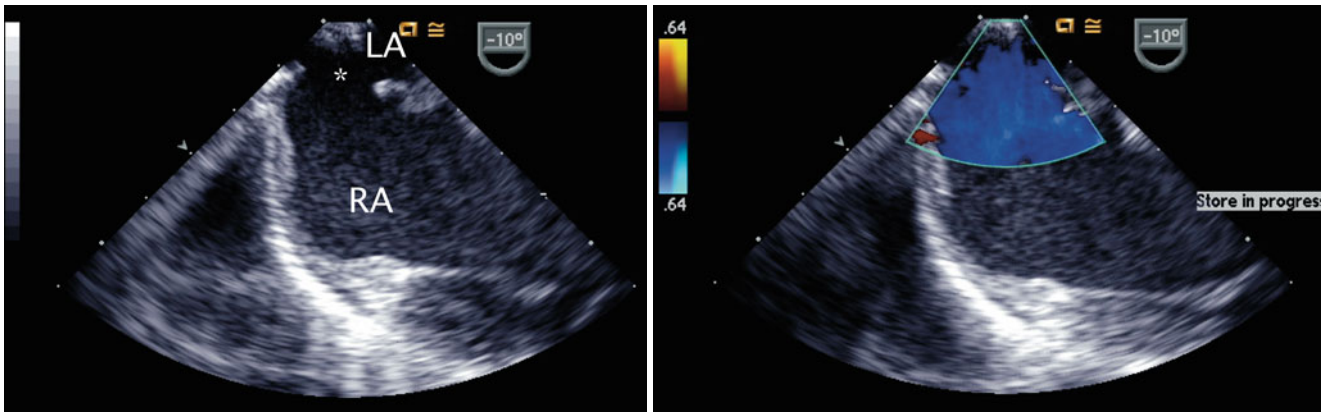

Fig. 7.5 *Left panel:* Superior sinus venosus atrial septal defect (*asterisk*) as seen by withdrawal of the imaging probe above the level of the fossa ovalis from a mid esophageal position. *Right panel:* Color Doppler imaging demonstrating flow across the defect. *LA* left atrium, *RA* right atrium

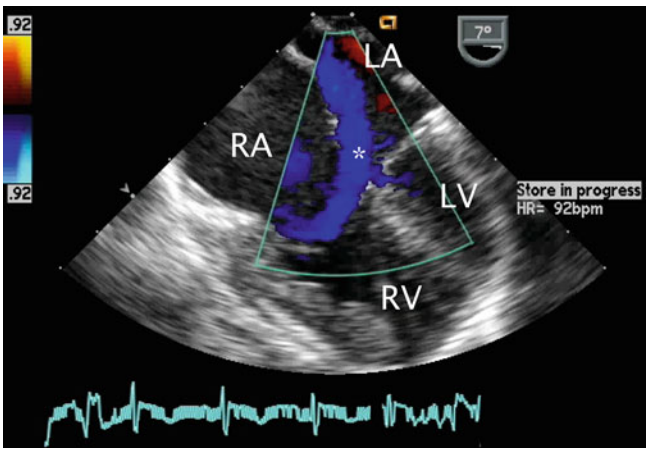

Fig. 7.6 Color Doppler image displaying left-to-right shunting across a primum atrial septal defect (*asterisk*) in the mid esophageal four chamber view. *LA* left atrium, *LV* left ventricle, *RA* right atrium, *RV* right ventricle

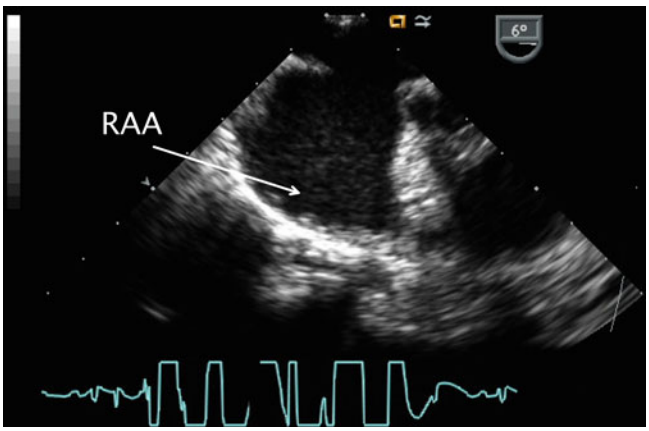

Fig. 7.7 Transesophageal image displaying the broad-based right atrial appendage (*RAA*). There is also a moderate to large secundum atrial septal defect present

of primum ASDs and Doppler interrogation of the atrioventricular valves (Fig. 7.6, Video 7.6; discussed in detail in Chap. 8).

Clockwise turning of the probe in the ME 4 Ch view visualizes the remainder of the RA. The proximal aspect of the right atrial appendage (RAA) can be seen with slight probe withdrawal (Fig. 7.7, Video 7.7), in addition to portions of the tricuspid valve and right ventricular inflow (Fig. 7.8, Video 7.8) with clockwise probe shaft rotation. Tricuspid valve inflow and the degree of tricuspid regurgitation can be assessed from this window as well as in the mid esophageal right ventricular inflow-outflow (ME RV In-Out) and transgastric right ventricular inflow (TG RV In) views. Determination of the Doppler peak velocity of tricuspid regurgitation can be used to estimate right ventricular and pulmonary artery systolic pressures. Pulmonary artery diastolic pressure may be predicted by measurement of theend-diastolic velocity of pulmonary regurgitation from the ME RV In-Out, mid esophageal aortic valve short axis (ME AV SAX), or deep transgastric sagittal (DTG Sagittal) views. Increased tricuspid valve inflow and pulmonary outflow Doppler velocities may be seen within the context of large ASDs with significantly increased pulmonary to systemic blood flow (Qp:Qs) ratios. Increased flow across these structures does not necessarily represent valvar stenosis and in most cases are regarded as 'flow-related gradients'. Pulmonary hypertension is quite rare, but may occur in patients with isolated ASDs over a period of many years.

Returning to the ME 4 Ch view, sometimes requiring slight further clockwise turning, as well as advancement or withdrawal of the probe, connection of the right pulmonary veins to the LA posteriorly can be demonstrated (Figs. 7.9 and 7.10, Videos 7.9 and 7.10; also refer to Chap. 6).

The sweep continues from the ME 4 Ch view with counterclockwise turning of the probe shaft to better visualize the LA (Fig. 7.11, Video 7.11). Probe advancement and retroflexion will enhance visualization of the coronary sinus and

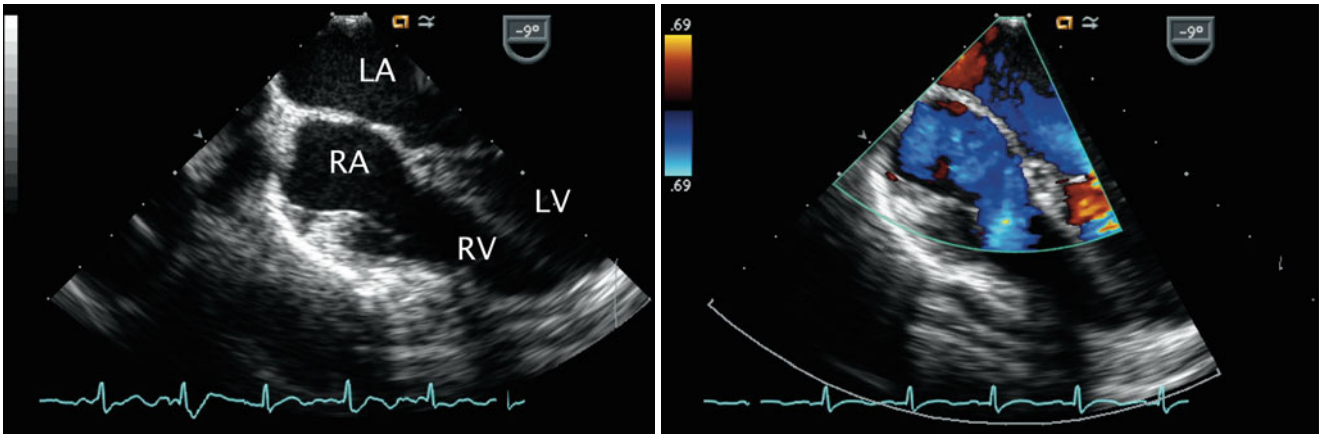

Fig. 7.8 *Left panel:* Image obtained by turning of the imaging probe from the mid esophageal four chamber view clockwise to visualize right-sided structures. *Right panel:* Color Doppler demonstrates an intact atrial septum and laminar tricuspid inflow in this example. *LA* left atrium, *LV* left ventricle, *RA* right atrium, *RV* right ventricle

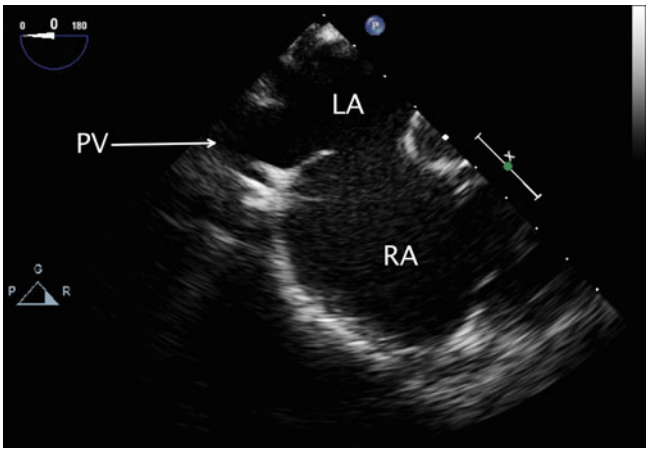

Fig. 7.9 Mid esophageal view with clockwise probe shaft rotation to examine the right pulmonary venous connections (*PV*) into the left atrium (*LA*). *RA* right atrium

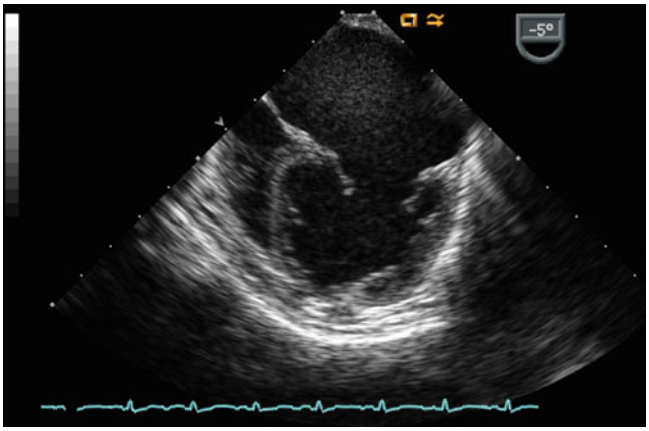

Fig. 7.11 Mid esophageal four chamber image obtained with counterclockwise rotation of the imaging probe demonstrates the left atrium (dilated due to mitral regurgitation in this example)

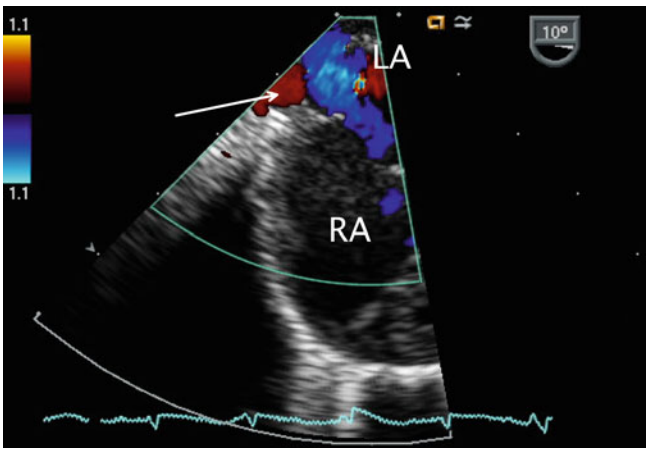

Fig. 7.10 Color flow Doppler in a similar plane as shown in Fig. 7.9 to assess drainage of the right upper pulmonary vein (*red color* flow shown by *arrow*) into the left atrium (*LA*). *RA* right atrium

identify areas of unroofing, if present. Continued further counterclockwise rotation of the probe in conjunction with advancement or withdrawal demonstrates the left pulmonary venous connections to the left atrial posterior-lateral wall (Fig. 7.12, Video 7.12). Color and pulsed wave Doppler can be applied to facilitate this assessment (Fig. 7.13, Video 7.13). Pulmonary vein stenosis, although rare in most uncomplicated ASDs, may be suggested by aliasing/turbulence by color Doppler (Fig. 7.14, Video 7.14). This finding should be confirmed by spectral Doppler interrogation. This view may demonstrate a dilated coronary sinus in cross section if a persistent left superior vena cava to coronary sinus connection is present (Fig. 7.15, Video 7.15). Anterior to the entry of the left pulmonary veins with slight probe withdrawal to nearly a ME AV SAX plane, the proximal portion of the left atrial appendage (LAA) can be seen from this window (Fig. 7.16, Video 7.16). Forward axial rotation of the

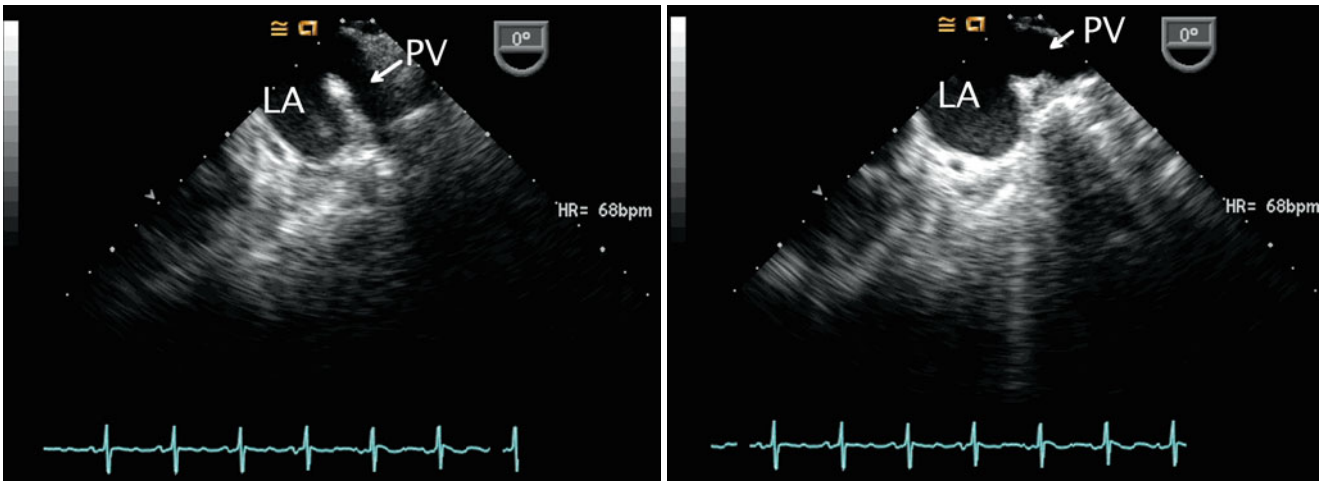

Fig. 7.12 The courses of two left sided pulmonary veins (*PV*) into the left atrium (*LA*) are demonstrated. *Left panel:* The left upper pulmonary vein is seen coursing in an anterior to posterior direction. *Right panel:* The more horizontal course of the left lower vein is demonstrated as it runs lateral to medial. Note the two different orientations of these veins as they enter the left atrium

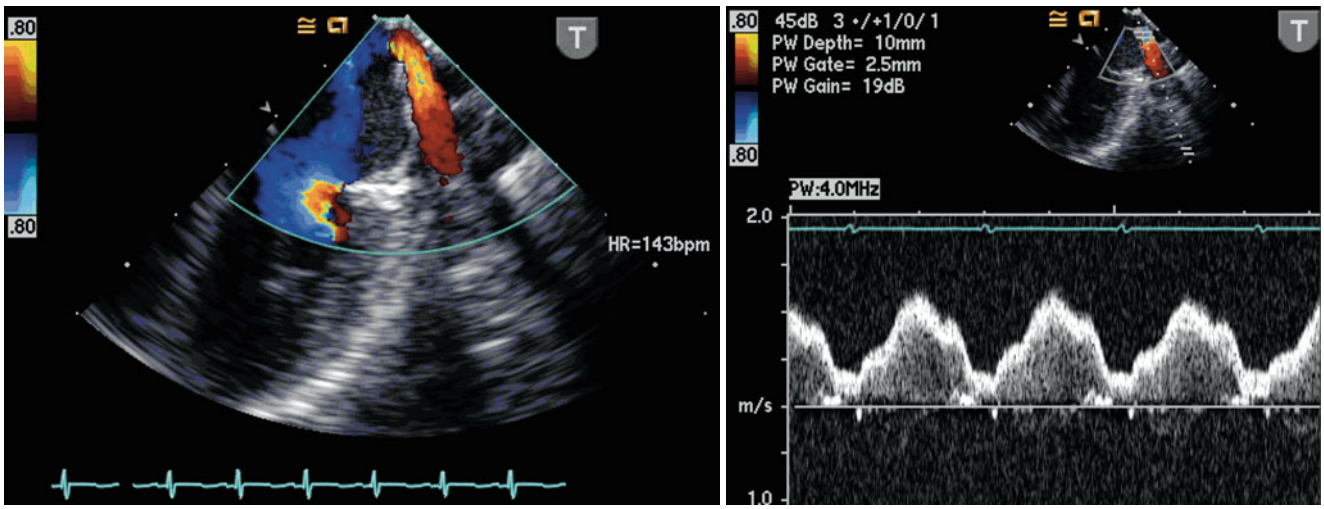

Fig. 7.13 Color flow Doppler imaging (*left panel*) and spectral tracing (*right panel*) complements the two-dimensional evaluation of the pulmonary veins. Note the characteristic normal systolic and diastolic nature of the pulmonary venous flow

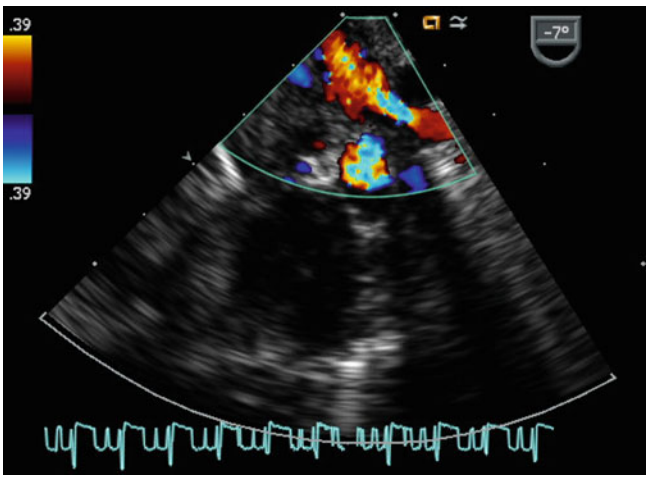

Fig. 7.14 Transesophageal color Doppler image of the left upper pulmonary vein as it courses towards the let atrium. Aliasing is seen by color flow interrogation that should prompt further investigation, including spectral Doppler interrogation

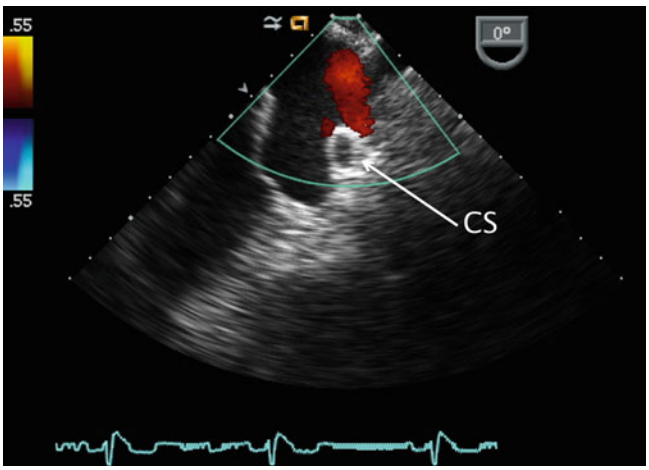

Fig. 7.15 Image displays a dilated coronary sinus (*CS, arrow*) as seen in cross-section (*arrow*) below the left pulmonary venous inflow. This may indicate the presence of a persistent left superior vena cava

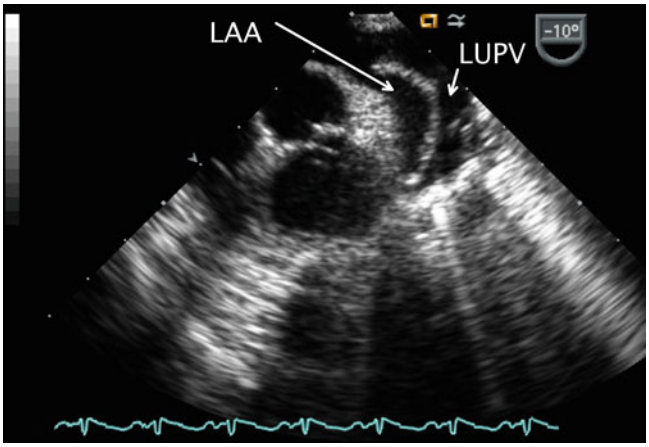

Fig. 7.16 Image obtained with transducer anteflexion as this is slightly withdrawn to a nearly mid esophageal aortic valve short axis plane. This cross-section displays the left atrial appendage (*LAA*) anteriorly located in relation to the left upper pulmonary vein (*LUPV*)

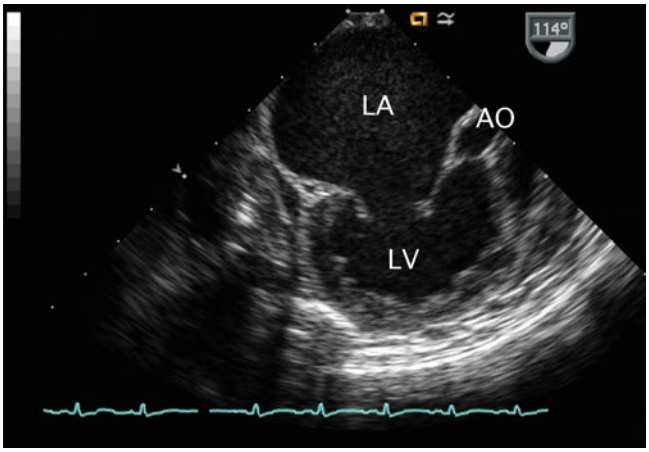

Fig. 7.18 Mid esophageal long axis view (multiplane angle 114°) corresponding to same patient displayed in Fig. 7.11. This image confirms the large dimensions of the left atrium (*LA*) and displays the left ventricle (*LV*) and aortic root (*AO*).

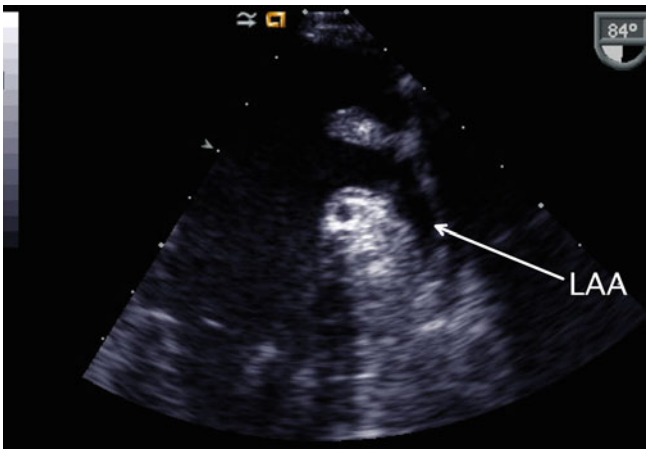

Fig. 7.17 Mid esophageal two chamber view demonstrating the anterior position (*arrow*) of the left atrial appendage (*LAA*)

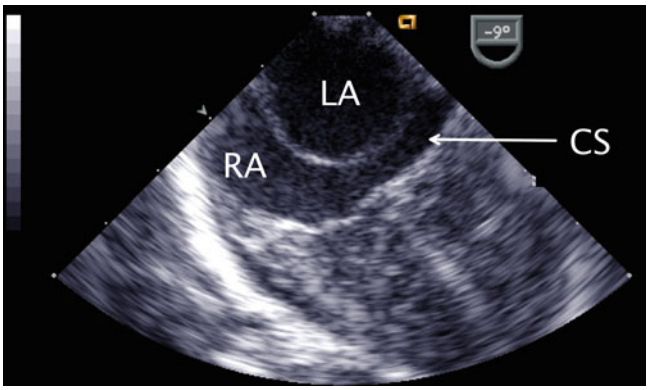

Fig. 7.19 Image obtained after slightly advancing the probe in the mid esophageal four chamber view. The coronary sinus (*CS*) in seen in long axis as it courses along the atrioventricular groove to drain into the right atrium (*RA*). *LA* left atrium

multiplane angle from the ME 4 Ch to the mid esophageal two chamber (ME 2 Ch) view (angle ~90°) displays the LA in an orthogonal plane and the LAA in long axis (Fig. 7.17, Video 7.17). Further counterclockwise turning of the TEE probe may visualize a left superior vena cava in long axis if one is present. From the ME 2 Ch plane forward transducer rotation displays a mid esophageal long axis (ME LAX) view (angle ~110°) and demonstrates the LA, mitral valve, and left ventricular outflow (Fig. 7.18, Video 7.18).

Slight advancement of the probe in the ME 4 Ch will allow for visualization successively of the coronary sinus as it courses longitudinally along the posterior atrioventricular groove (Fig. 7.19, Video 7.19), along with the coronary sinus orifice as it normally drains into the RA, and the lower portion of the interatrial septum. This is also the area where deficiency of atrial septal tissue surrounding the coronary sinus orifice on the RA may be identified in patients with a coronary sinus-type ASD. A dilated coronary sinus should not be confused for a primum ASD. Agitated saline injection into a left arm vein or left jugular vein will demonstrate contrast in the coronary sinus and drainage into the RA if a persistent left superior vena cava to coronary sinus connection is present (Fig. 7.20, Video 7.20) (Chap. 6).

From the ME 4 Ch view, clockwise turning of the probe and forward angle rotation displays the mid esophageal bicaval (ME Bicaval) view, angle ~90°–110°. This provides an excellent cross-section of the entire atrial septum (superior to inferior) (Figs. 7.21 and 7.22, Videos 7.21 and 7.22). The majority of the interatrial septum will be oriented optimally with respect to 2D and Doppler imaging from this view. This window is ideal for confirming the presence of superior (Fig. 7.23, Video 7.23) and inferior sinus venosus defects,

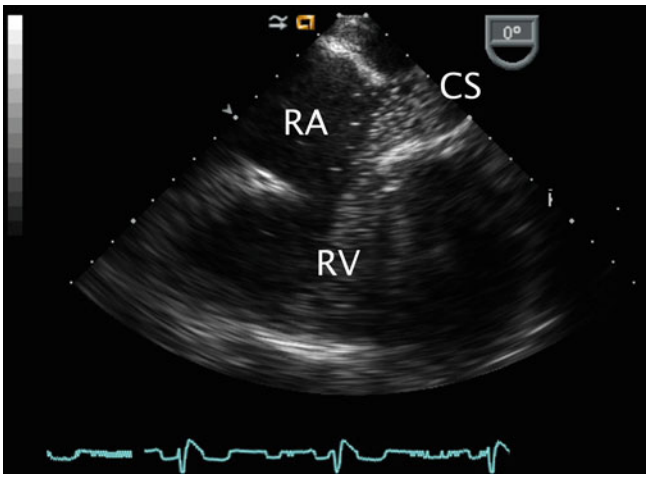

Fig. 7.20 Injection of agitated saline into a left arm vein in a patient with a persistent left superior vena cava demonstrating contrast in the coronary sinus (*CS*) thus confirming the connection. *RA* right atrium, *RV* right ventricle

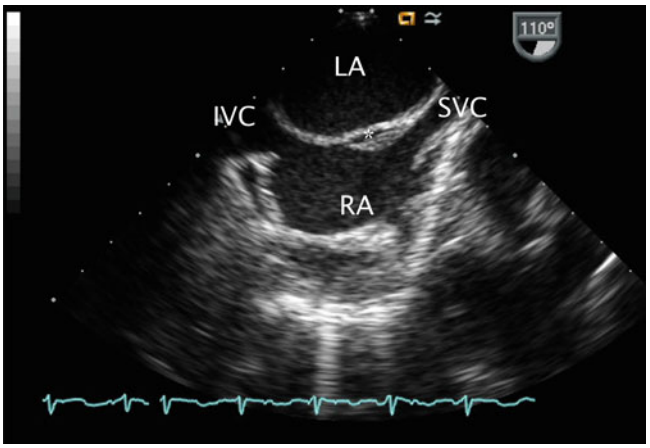

Fig. 7.21 Mid esophageal bicaval view displaying the entire atrial septum. The flap valve of the foramen is well seen (*asterisk*). *IVC* inferior vena cava, *LA* left atrium, *RA* right atrium, *SVC* superior vena cava

secundum defects (Figs. 7.24, 7.25, and 7.26, Videos 7.24, 7.25, and 7.26), and a PFO [42–44]. As mentioned, contrast echocardiography with a Valsalva (or simulated Valsalva maneuver during mechanical ventilation) may be required for the detection of shunting across a PFO.

Slight clockwise/counterclockwise probe turning from the ME Bicaval view may be necessary to optimally visualize an ASD depending upon its size and location. Withdrawal of the probe while in this view displays the superior vena cava in long axis. Probe advancement provides long axis imaging of the inferior vena cava (Fig. 7.22, Video 7.22). Anomalous pulmonary veins entering either vena cavae may be seen from these views with appropriate probe withdrawal and/or advancement (Fig. 7.27, Video 7.27)

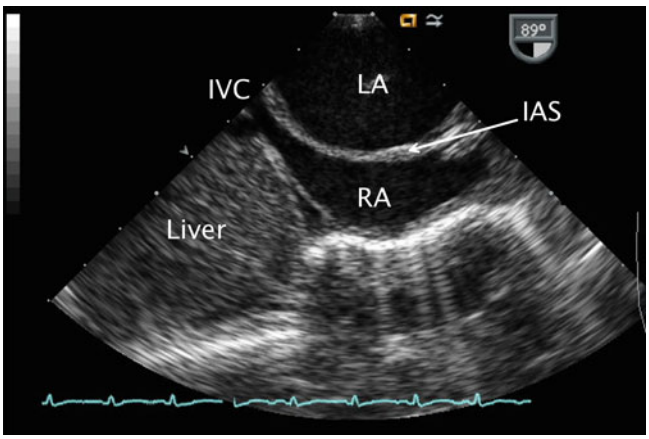

Fig. 7.22 Image of a mid esophageal bicaval view displaying a dilated left atrium (*LA*) with bulging of the interatrial septum (*IAS*) towards the right atrium (*RA*). The inferior vena cava (*IVC*) is also seen in this view it enters the RA

While in the ME 4 Ch view, advancement of the probe displays the lower esophageal situs short axis (LE Situs SAX) view. The junction of the inferior vena cava into the RA and upper portion of the vena cava can be seen in this cross-section. Further clockwise turning of the probe may be necessary during this sweep. This view can also be useful in the assessment of inferior vena cava-type of sinus venosus defects and anomalous pulmonary veins entering the vena cava.

Forward axial rotation of the imaging probe through the ME RV In-Out view (angle ~60°), allows more complete anatomic assessment of the tricuspid valve, right atrial, and ventricular size, and right ventricular outflow tract and pulmonary valve. This view is particularly helpful to demonstrate right ventricular volume overload and systolic function (Fig. 7.28, Video 7.28) in the setting of communications at the atrial level. The transgastric mid short axis (TG Mid SAX) view also provides information regarding right ventricular size and magnitude of atrial level shunting in these lesions (Fig. 7.29, Video 7.29).

Further views of the interatrial septum can also be obtained from the deep transgastric window. Once the DTG Sagittal view is obtained (angle ~90°–100°) clockwise probe rotation as necessary allows for the entire interatrial septum to be displayed; the multiplane angle can be adjusted for optimal visualization of the atrial septum (Figs. 7.30, 7.31, and 7.32, Videos 7.30, 7.31, and 7.32). The deep transgastric windows complement the assessments of ASDs (Fig. 7.33, Video 7.33) and in some cases allow for details of the anatomy not visualized in other views to be demonstrated.

Evaluation of right atrial and right ventricular size, which generally reflect the relative volume of left-to-right shunting through an ASD, provides a qualitative assessment of the clinical significance of the defect. Pertinent TEE windows

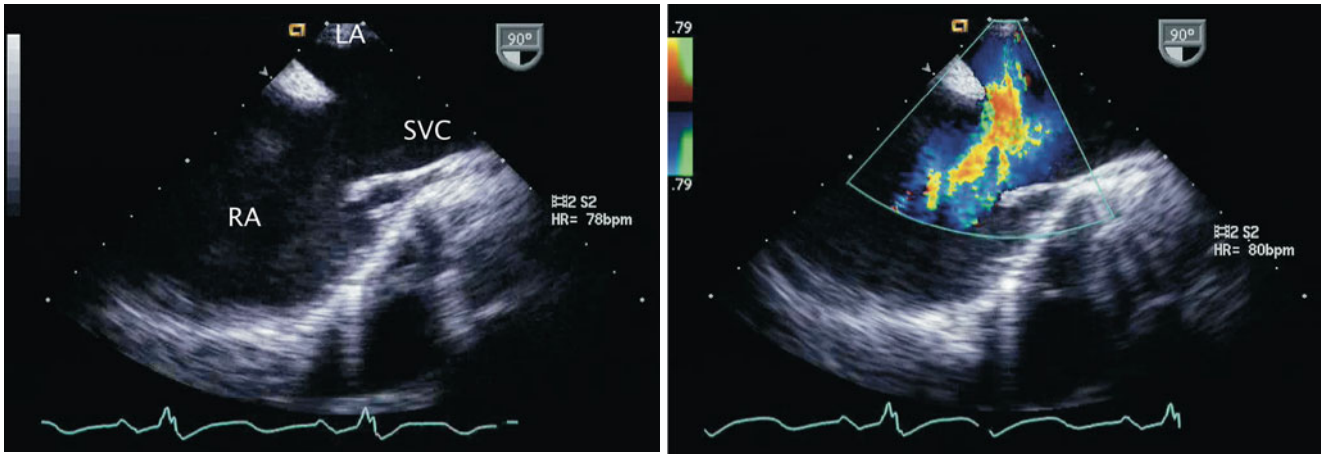

Fig. 7.23 *Left panel:* Two-dimensional image of a superior sinus venosus defect in the mid esophageal bicaval view. The superior vena cava (*SVC*) frequently straddles the interatrial septum in this defect. *Right panel:* Color flow Doppler confirms left-to-right shunting across the atrial communication. *LA* left atrium, *RA* right atrium

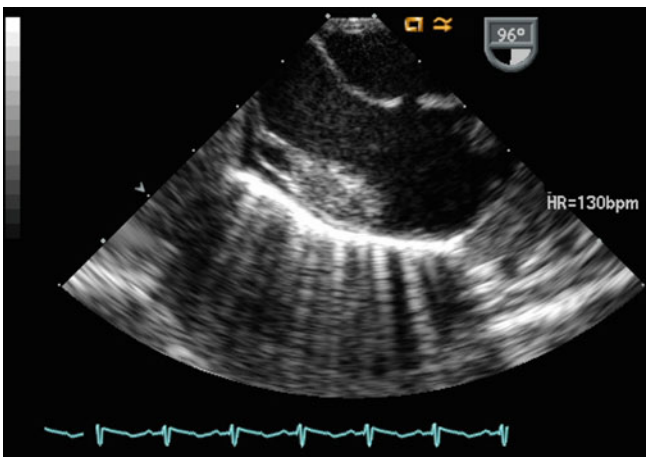

Fig. 7.24 Small secundum atrial septal defect as shown in the mid esophageal bicaval view

include: at the mid esophageal level the 4 Ch, RV In-Out and Bicaval views (Fig. 7.34, Video 7.34); at the transgastric level the RV In, Basal SAX, and Mid SAX views; and at the deep transgastric window the DTG Sagittal view and modified cross-sections. Qualitative assessment of right and left ventricular systolic function and color and spectral Doppler evaluation of associated lesions, as appropriate, are also indicated. Normal biventricular systolic function with flattening of the interventricular septum in diastole is a common finding in defects resulting in right ventricular volume overload.

The considerations in the echocardiographic assessment of atrial level communications are summarized in Table 7.1.

Surgical and Transcatheter Considerations

Preprocedure Assessment

Preoperative TEE evaluation focuses on confirming the size and location of the ASD, exclusion of additional congenital cardiac lesions, and assessment of atrial and ventricular chamber size and ventricular systolic function. Pulmonary venous anatomy should be evaluated, particularly in patients with sinus venosus ASDs. Care should be taken not to mistake a redundant Eustachian valve in the RA for the atrial septum and potentially misdiagnose an ASD that does not exist. Likewise, as discussed, a dilated coronary sinus should not be interpreted to represent a primum-type communication. Doppler evaluation of the atrial shunt and quantitation of the degree and peak velocity of tricuspid regurgitation should be performed.

In patients with a secundum ASD or PFO deemed suitable for transcatheter device closure, TEE evaluation includes size and location of the communication, evaluation of adequacy of atrial septal tissue rims (particularly the retroaortic rim), exclusion of additional septal defects, evaluation for atrial septal aneurysm (Fig. 7.35, Video 7.35), and assessment of ventricular chamber size and function [45–50]. The relationship of the defect to the vena cavae and atrioventricular valves and balloon sizing of the ASD or tunnel length of the PFO for suitable device selection are also important features to be evaluated. These considerations are discussed in detail Chap. 17.

For some severe forms of CHD, an ASD is actually necessary to maintain a physiology compatible with survival. In these types of patients, restrictive or non-existent atrial communications may require catheter-based interventions. These are aimed at either creating or enlarging an atrial communication allowing for either enhanced mixing of systemic and pulmonary venous blood (e.g. d-transposition of the great arteries) or decompression of venous return typically in cases of atrioventricular valve stenosis or atresia (Fig. 7.36, Video 7.36). These interventions might also benefit from TEE guidance, particularly in infants, as this patient group may be quite ill. TEE may limit radiation exposure and enhance the safety of these procedures.

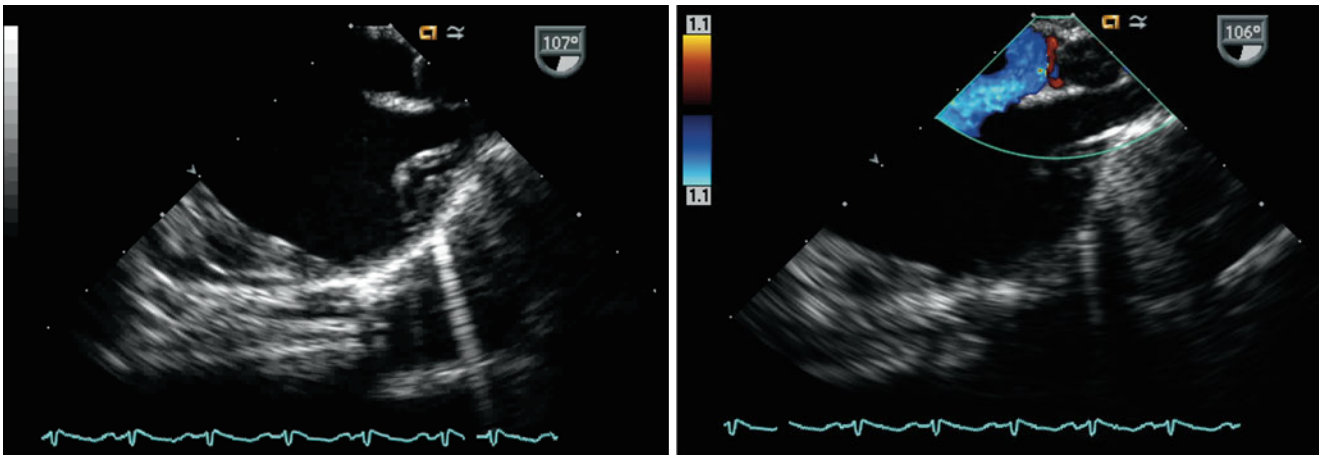

Fig. 7.25 Images demonstrate a high secundum atrial septal defect in the mid esophageal bicaval view (*left panel*) and corresponding color flow Doppler (*right panel*)

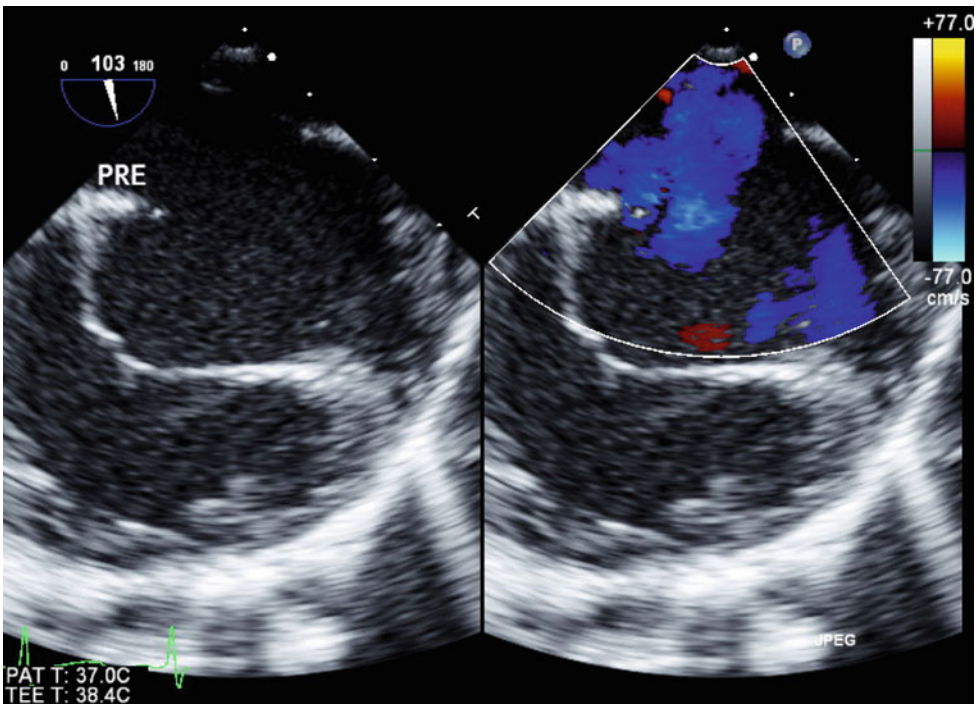

Fig. 7.26 Large secundum atrial septal defect (*left panel*) with associated left-to-right shunting (*right panel*). Note the slightly more inferior location of this defect as compared to the communication illustrated in a similar imaging plane in Fig. 7.25

Postprocedure Assessment

Postoperative evaluation following surgical closure of an ASD begins with confirmation of adequate cardiac de-airing. Evaluation of the surgical repair involves exclusion of residual atrial level shunting (Figs. 7.37 and 7.38, Videos 7.37 and 7.38), quantification of atrioventricular valve regurgitation, and assessment of ventricular systolic function following weaning from cardiopulmonary bypass. In surgeries involving closure of sinus venosus ASDs with redirection of anomalous pulmonary veins it is very important to exclude vena caval or pulmonary venous obstruction post repair [51–53].

TEE is useful for ASD/PFO occlusion device positioning and during deployment confirms the adequacy of device position after release. Postdevice evaluation includes: (1) assessment of residual shunting, (2) evaluation of the vena cava and right pulmonary veins to exclude impingement of the device into these structures, and (3) Doppler assessment of atrioventricular valve inflow and regurgitation, and aortic valve regurgitation (particularly in cases with small retroaortic septal rims where the device arms straddle the aortic root). Ventricular systolic function should also be evaluated. Also refer to Chap. 17 for an in depth discussion of this subject.

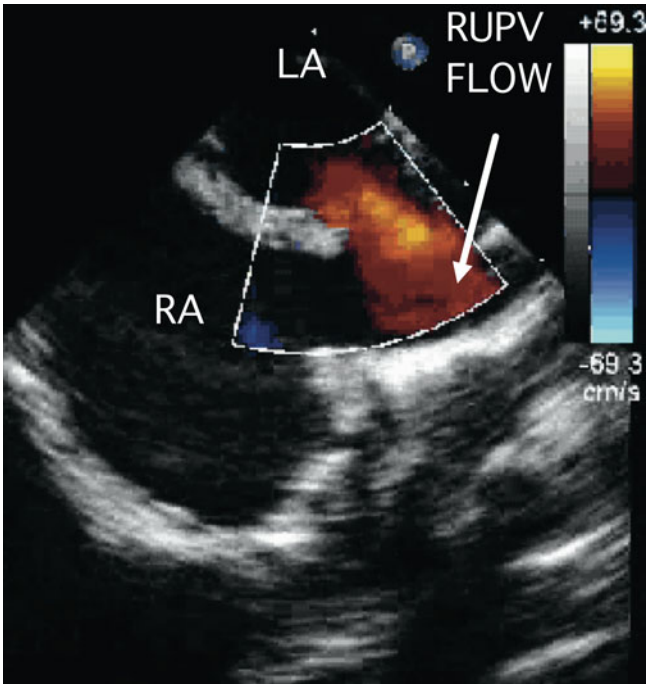

Fig. 7.27 Image demonstrates flow from the right upper pulmonary vein (*RUPV*) directed towards the superior vena cava-right atrial junction in a superior sinus venosus defect. *LA* left atrium, *RA* right atrium. Image courtesy of Thomas M. Burch, MD

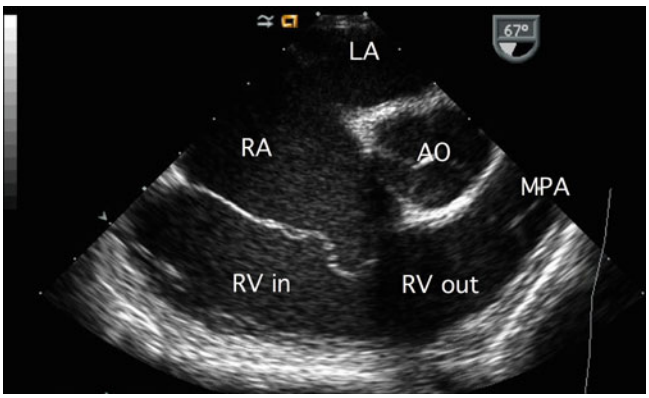

Fig. 7.28 Image of a mid esophageal right ventricular inflow-outflow view. This cross-section is useful in the comprehensive assessment of atrial septal defects as it displays the tricuspid valve, left atrium (*LA*), right atrial (*RA*) and right ventricular (*RV*) sizes, right ventricular inflow (*RV in*) and outflow (*RV out*) tract, pulmonary valve, and proximal main pulmonary artery (*MPA*). *AO* aorta

Juxtaposition of the Atrial Appendages

The atrial appendages normally lie on opposite sides of the roots of the great arteries. Juxtaposition of the atrial appendages, in which both appendages are oriented side by side on either the right ("right juxtaposition"), or much more commonly on the left ("left juxtaposition") was first described in 1954 [54]. This atrial anomaly is quite rare (found in ~0.8 % of congenital heart lesions). In most cases the atria are otherwise usually arranged (rarely, it is seen in left atrial isomerism) [55, 56]. Left juxtaposition is generally felt to be more

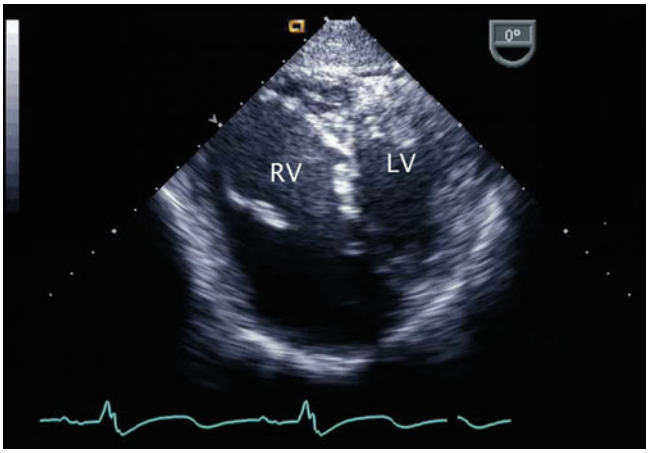

Fig. 7.29 Transgastric mid short-axis view demonstrating a large, volume loaded right ventricle (*RV*) in a patient with a large atrial septal defect. *LV left ventricle*

significant clinically [57, 58]. Juxtaposition of the atrial appendages is generally not seen in isolation, usually being found in conjunction with other complex congenital cardiac lesions, with left juxtaposition most commonly found in association with cyanotic conditions such as transposition of the great arteries, tricuspid atresia, and heterotaxy syndromes [55, 56, 59–61]. There is often some degree of hypoplasia of the right heart structures. Right juxtaposition has been described in conjunction with double outlet right ventricle and ventricular septal defect [61]. Although not hemodynamically significant *perse*, juxtaposition of the atrial appendages may have implications for catheter-based interventions as well as surgical procedures. Juxtaposed atrial appendages may be confused with an ASD if the abnormal septal configuration is not recognized [62–64].

Non invasive diagnosis of left juxtaposition of the atrial appendages is possible by TTE, however it represents a challenging diagnosis requiring a high level of suspicion [65]. Echocardiographic features include: (1) abnormalities of the plane of the atrial septum and (2) direct visualization of the abnormally oriented atrial appendage coursing anterior to the atria and posterior to the great arteries. TEE can provide further anatomic confirmation of this lesion in most cases [60].

Transesophageal Echocardiographic Evaluation

An important consideration in the TEE evaluation of this anomaly is recognition of the characteristic morphologic features of the atrial appendages and the normal orientation of the atrial septum [66]. Normally, the RAA is broad-based and displays a triangular shape (Fig. 7.7, Video 7.7), whereas the LAA is narrow-based relative to the remainder of the atrium and has an elongated shape (Fig. 7.16, Video 7.16). The abnormal orientation of the appendages in juxtaposition can be suspected/confirmed by recognizing these unique morphologies. In addition the abnormal orientation of the

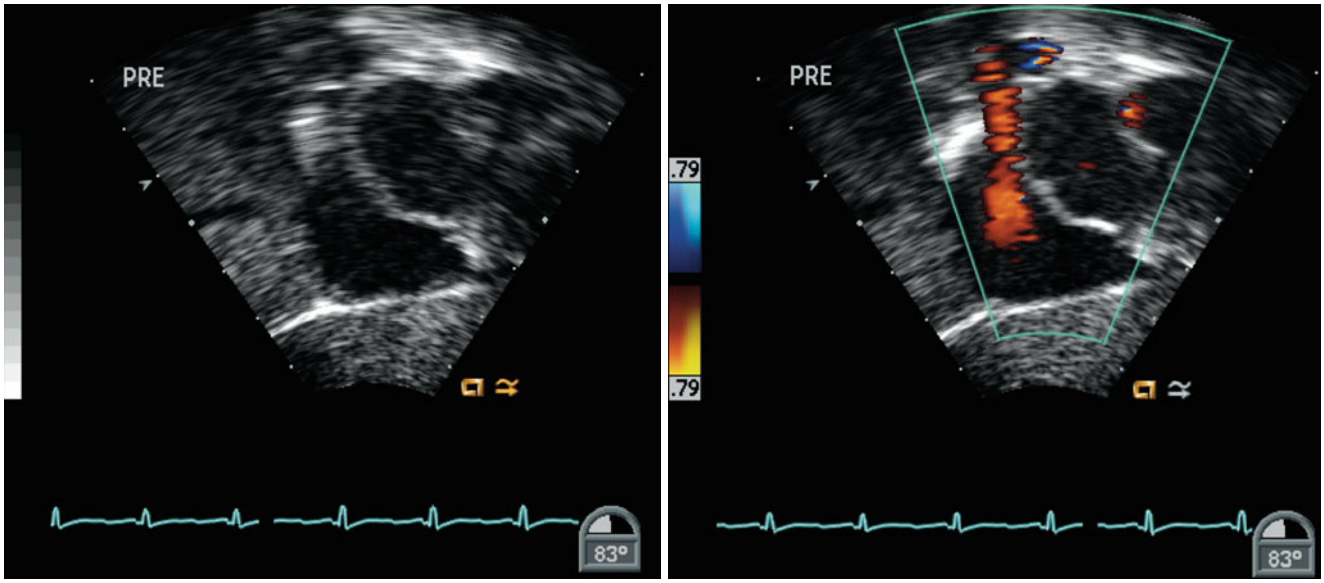

Fig. 7.30 Deep transgastric sagittal images of the atrial septum displaying two-dimensional (*left panel*) and color information (*right panel*). The interatrial septum appears intact by two-dimensional imaging

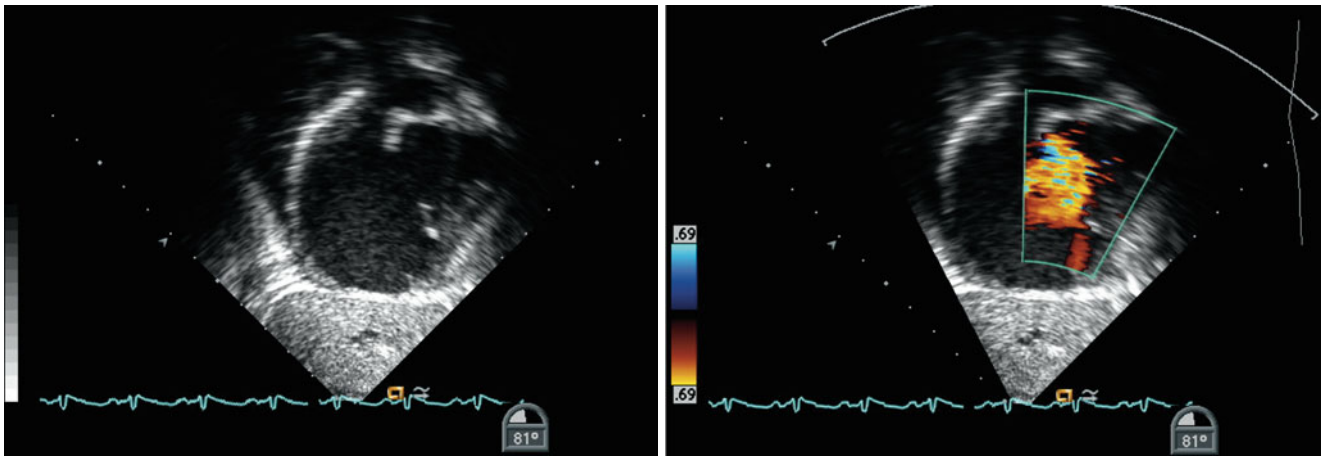

Fig. 7.31 Images obtained in the same cross-sections as shown in Fig. 7.30. In this example, the presence of a secundum atrial septal defect is demonstrated

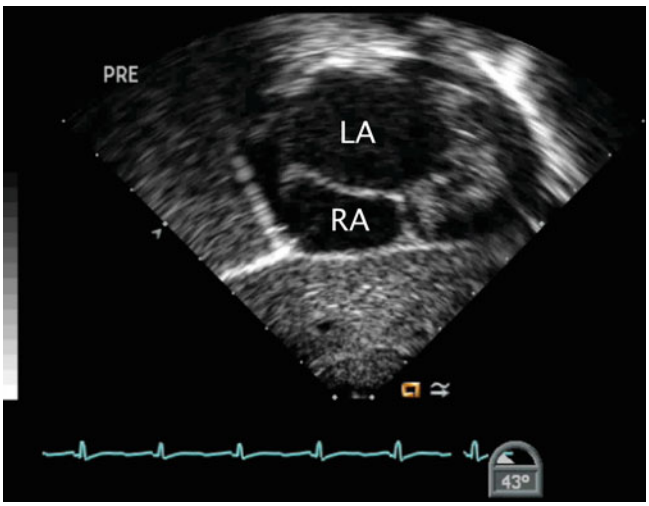

Fig. 7.32 The image displays a modified plane in the deep transgastric window that also allows for echocardiographic assessment of the interatrial septum. *LA* left atrium, *RA* right atrium

interatrial septum may provide a clue. The characteristic findings in left juxtaposition of the atrial appendages are lateral deviation of the posterior portion of the atrial septum (Fig. 7.39, Video 7.39) and a right to left horizontal (frontal) orientation of the antero-superior portion of the atrial septum that forms the posterior wall of the junction of the RAA with the atrial cavity [60]. These features are best demonstrated from several views.

The atrial septum is well seen from ME 4 Ch view, which in this anomaly would display the frontal deviation of the superior septum and opening of the left-deviated RAA behind the posterior great artery and anterior to the body of the LA (Fig. 7.40, Video 7.40). It should be emphasized that assessment of this anomaly in the ME 4 Ch view requires sweeps spanning multiple planes from the posterior to the anterior aspect of the heart. The characteristic echocardiographic features of juxtaposed appendages can also be seen

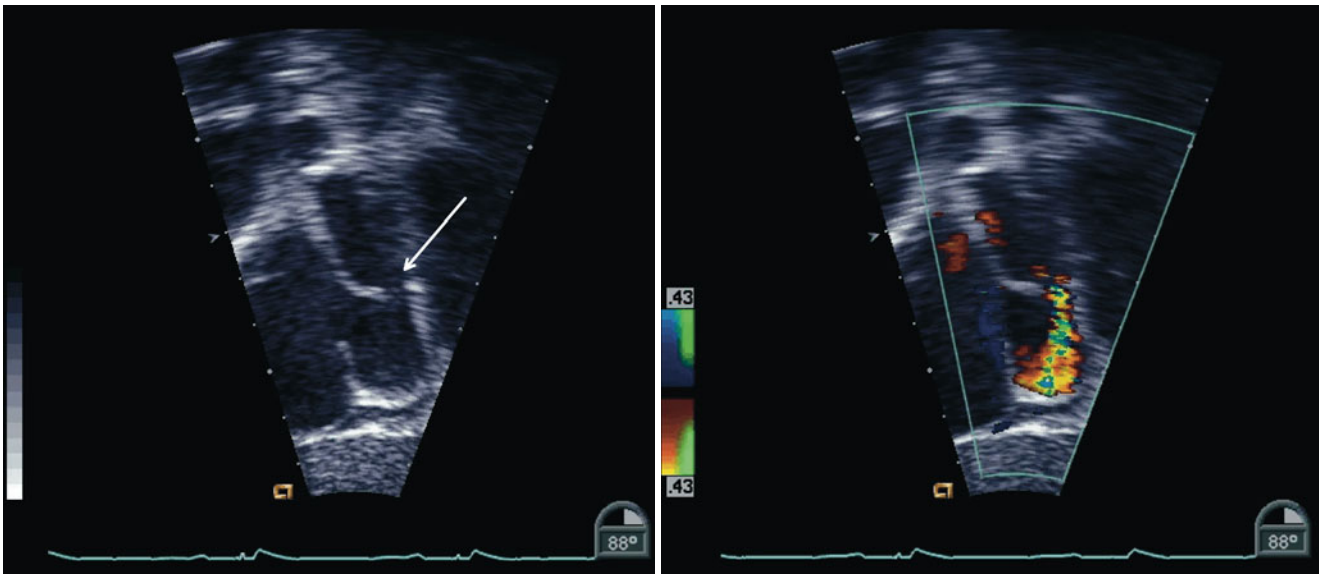

Fig. 7.33 Images of an inferior sinus venosus defect as obtained from a modified deep transgastric sagittal view (same view as shown in Figs. 7.30 and 7.31). Note the deficiency (*arrow*) in the inferior aspect of the interatrial septum (*left panel*) and the presence of left-to-right shunting across this region (*right panel*). The Eustachian valve is also seen. Additional planes in this window may provide information regarding associated anomalies of pulmonary venous drainage

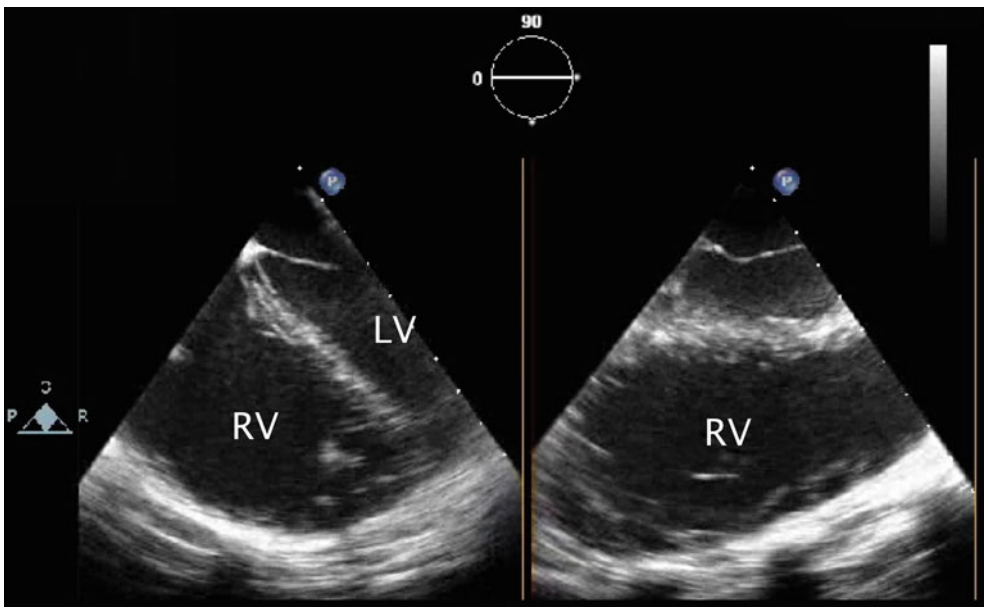

Fig. 7.34 Mid esophageal images in orthogonal planes that assist in the determination of right ventricular (*RV*) size and function. Moderate right ventricular dilation is shown. (*LV*) left ventricle

as the imaging probe is slowly withdrawn from the ME 4 Ch, multiplane angle axially rotated forward and adjusted between the ME AV SAX and mid esophageal ascending aortic short axis (ME Asc Ao SAX) views. Slight anteflexion of the probe may be helpful. In the ME RV In-Out view the RAA can also be demonstrated coursing behind the posterior great artery and anterior to the LA.

From the ME 4 Ch view, clockwise probe shaft rotation and forward axial rotation to an angle ~90°–95° displays the entire atrial septum as visualized in the ME Bicaval view. The characteristic septal malalignment, with posterior deviation of the superior portion and anterior deviation of the inferior portion can be also seen from this view. The ME LAX and mid esophageal ascending aorta long axis (ME Asc Ao LAX) views can also demonstrate the RAA behind the posterior great artery and anterior to the LA.

Probe withdrawal from a TG Basal SAX/LE Situs SAX planes with anteflexion may demonstrate the appendage crossing behind the great arteries. Further views of the interatrial septum displaying the septal malalignment and opening of the abnormally oriented atrial appendage can also be obtained from the deep transgastric views with clockwise/

Table 7.1 Atrial communications

Summary of important considerations for TEE assessment
Anatomy of the atrial septal defect or patent foramen ovale
Size and location of defect (single versus fenestrated)
Septal rims
Septal anatomy
Direction of atrial level shunt
Drainage of pulmonary veins
Atrial chamber size
Doppler assessment of atrioventricular valves (regurgitation); mitral valve anatomy (prolapse, cleft)
Assessment for possible pulmonary hypertension
Estimation of right ventricular systolic pressure by tricuspid regurgitation jet velocity
Estimation of right ventricular diastolic pressure by pulmonary regurgitation end-diastolic velocity
Identification and evaluation of other associated congenital cardiac lesions
Ventricular chamber size and systolic function

counterclockwise adjustments as necessary and anterior to posterior sweeping (Fig. 7.41, Video 7.41). Evaluation of associated defects (particularly transposition of the great arteries, tricuspid valve obstructive lesions, and ASDs) should also be undertaken as indicated.

Color and pulsed-wave Doppler can help to distinguish between flow across an ASD and flow in an atrial appendage in cases where 2D imaging is inconclusive. Tricuspid valve obstructive lesions other than atresia can co-exist with other complex congenital heart defects, particularly transposition of the great arteries thus careful Doppler evaluation of the tricuspid valve is warranted. Color flow Doppler can facilitate identification of an associated ASD, which may have a more anterior opening due to the abnormal septal configuration. Appropriate Doppler evaluation of any additional associated lesions and routine assessment of ventricular function are also indicated. Finally, thrombi can form in a juxtaposed appendage and should be assessed for [67].

Salient features of the echocardiographic evaluation of juxtaposed atrial appendages are summarized in Table 7.2.

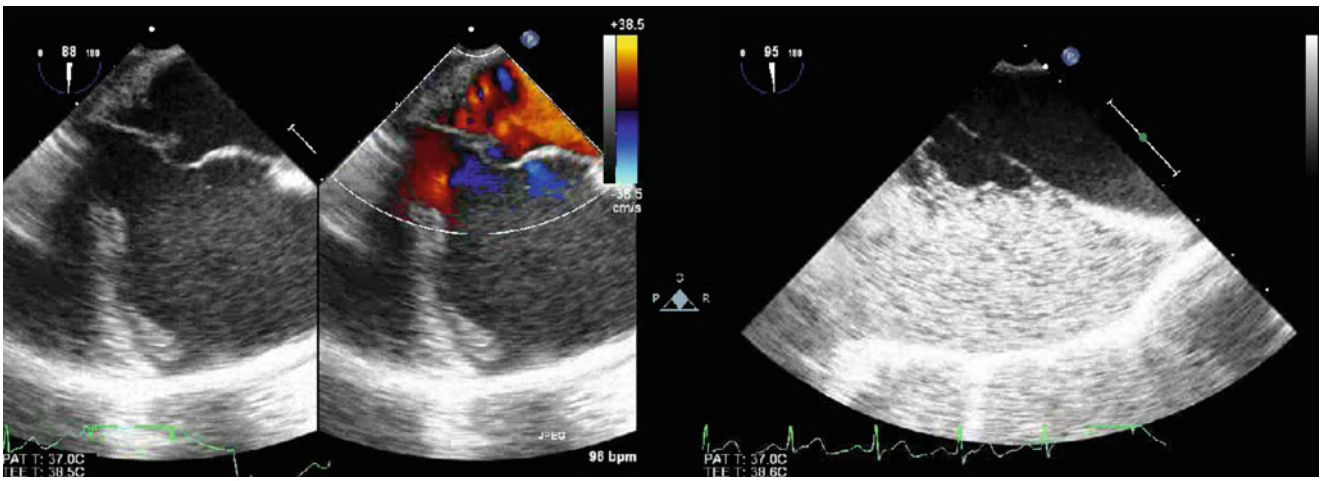

Fig. 7.35 Images demonstrate an aneurysm of the interatrial septum as shown by two-dimensional imaging (*left panel*), color flow mapping (*middle panel*), and contrast echocardiography (*right panel*). Injection of agitated saline into a lower extremity vein was performed to assess for the presence of a patent foramen ovale in a child with a history of multiple strokes

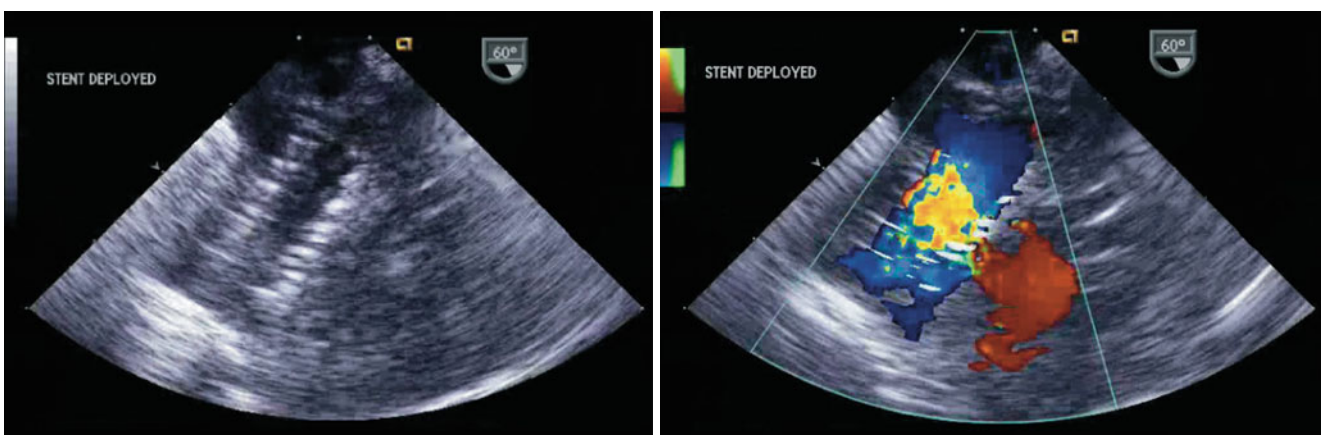

Fig. 7.36 *Left panel:* Two-dimensional image of an atrial septal stent placed following radiofrequency perforation of the interatrial septum in a critically ill infant with hypoplastic left heart syndrome and an intact atrial septum. *Right panel:* Color Doppler depicts flow across the central aspect of the stent

Surgical and Transcatheter Considerations

Juxtaposed atrial appendages may be found incidentally at the time of surgical intervention for other complex heart defects. This anomaly usually has little impact on outcome in the present surgical era. Atrial baffle procedures (Senning or Mustard), which are rarely performed today, could conceivably be complicated by this anomaly. On occasion this may influence a Fontan connection or atrial cannulation for cardiopulmonary bypass. However, the associated lesions generally have much greater surgical implications than the juxtaposed appendages [59].

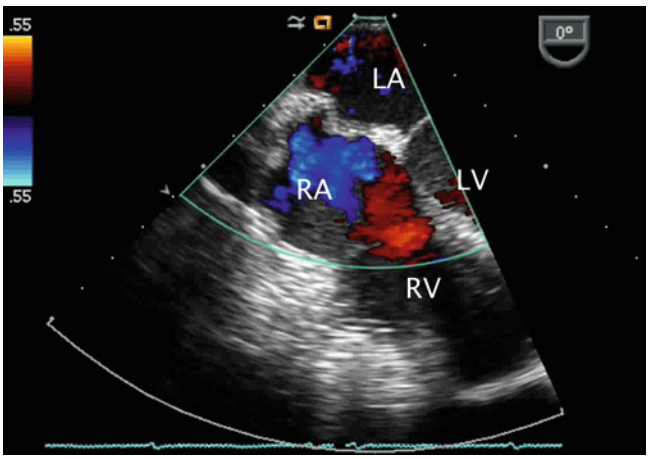

Fig. 7.37 Mid esophageal four chamber imaging with color flow interrogation to assess the results of the surgical intervention following patch closure of a secundum atrial septal defect. *LA* left atrium, *LV* left ventricle, *RA* right atrium, *RV* right ventricle

Although not usually a setting where TEE is routinely utilized, a more important consideration worth mentioning concerns performance of balloon atrial septostomy in patients with *d*-transposition of the great arteries and left juxtaposition of the atrial appendages. An increased risk of inadvertent placement of the balloon catheter tip into the abnormally oriented RAA has been reported that, if not recognized, can lead to complications during attempted septostomy. The combination of 2D imaging and Doppler interrogation may avoid mistaking the base or mouth of a juxtaposed RAA for an atrial communication in this instance. In addition, recognition of the abnormal atrial septal configuration and the often unusual placement/orientation of the ASD/PFO in this anomaly by TEE can assist in catheter manipulation, save valuable time, and potentially increase the margin of safety of the procedure. This may be important in clinically unstable, cyanotic neonates in whom time is of the essence.

Cor Triatriatum

Cor triatriatum consists of a congenital fibromuscular membrane dividing either the RA or LA into proximal (venous) and distal (atrial) chambers. The term "cor triatriatum", when used alone, usually refers to a left atrial membrane, also sometimes called "cor triatriatum sinister". Although by far the most common form of the defect, this is a rare cardiac anomaly, accounting for less than 2–4 % of all congenital heart disease. An even less common form of this lesion may affect the RA (cor triatriatum dexter) and will not be discussed in depth.

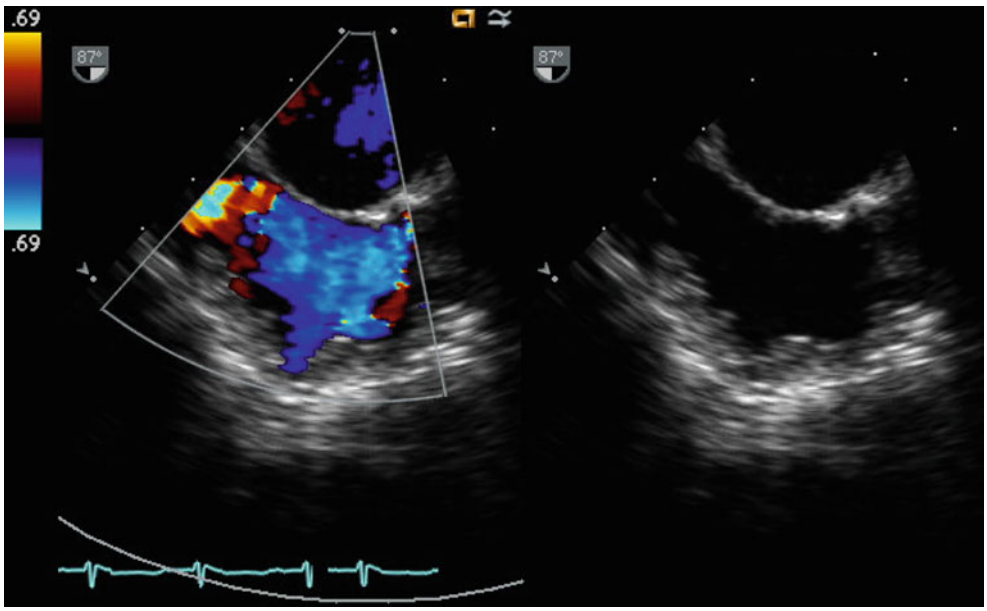

Fig. 7.38 Images display the post surgical evaluation of a secundum atrial septal defect in the mid esophageal bicaval plane. No residual shunting is detected across the patch

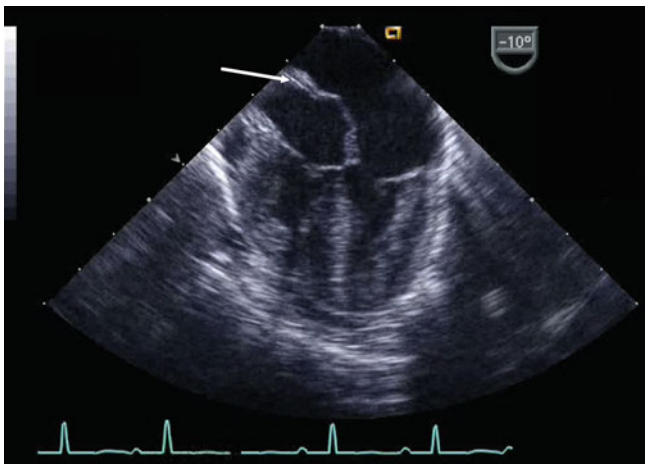

Fig. 7.39 Note the abnormal orientation (*arrow*) of the interatrial septum in a patient with juxtaposed left atrial appendages

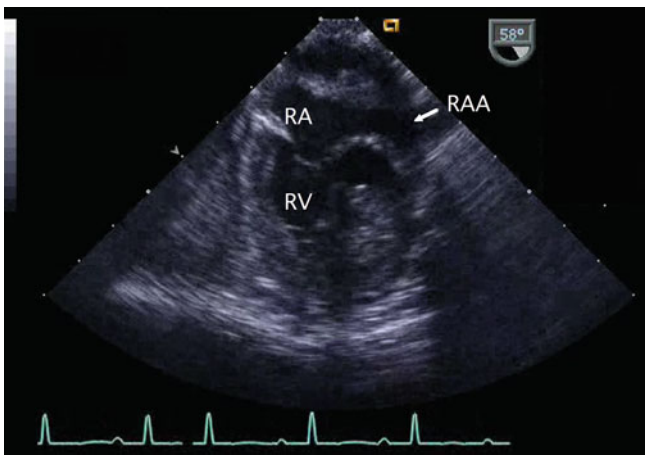

Fig. 7.40 Image displays the abnormal position of the right atrial appendage (*RAA*) as it extends from the right atrium (*RA*) to lie next to the left atrial appendage in left juxtaposition of the atrial appendages. The abnormal orientation of the interatrial septum is also appreciated in this view. *RV* right ventricle

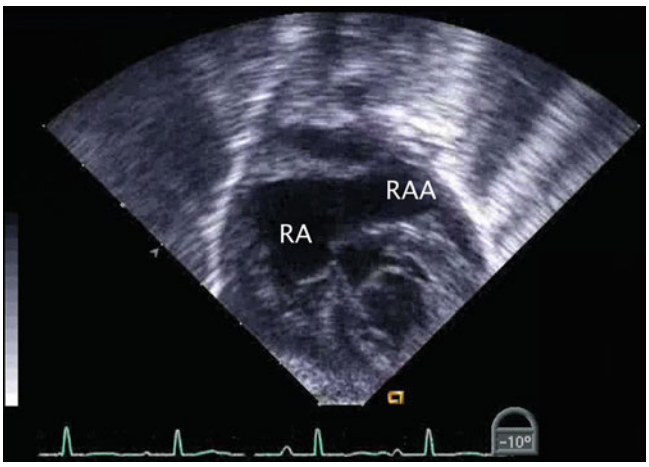

Fig. 7.41 This deep transgastric image further displays the anatomy/orientation of the atrial appendages in the infant shown in Figs. 7.39 and 7.40 with juxtaposition of the atrial appendages. Note the position of the right atrial appendage (*RAA*) on the *left side* (left juxtaposition). Associated defects in this patient included double outlet right ventricle/malposed great arteries (Taussig Bing Anomaly). *RA* right atrium

Table 7.2 Juxtaposition of atrial appendages

Summary of important considerations for TEE assessment
Anatomy of the juxtaposed atrial appendage
Right versus left juxtaposition
Identification and evaluation of other associated congenital cardiac lesions
Left juxtaposition
Transposition of the great arteries, tricuspid stenosis/atresia
Heterotaxy syndrome, left atrial isomerism
Right juxtaposition
Ventricular septal defects, double outlet right ventricle
Other
Atrial septal defects
Thrombi

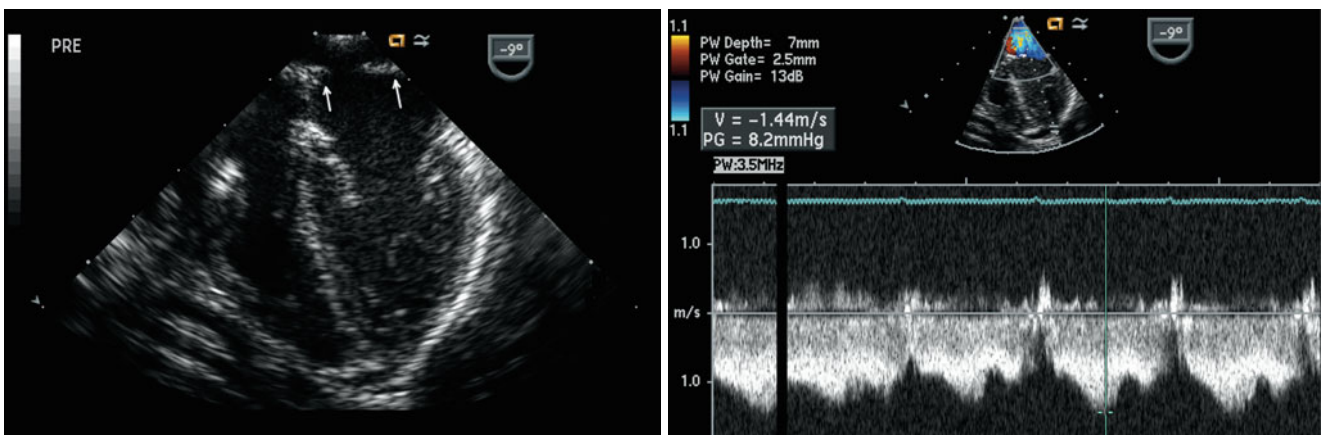

Fig. 7.42 *Left panel:* Mid esophageal view depicting a cor triatriatum membrane (*arrows*). *Right panel:* Spectral Doppler analysis across the orifice of the membrane is performed to determine the severity of obstruction. Although a peak velocity is measured in this tracing, parameters considered more representative of the degree of obstruction include the mean gradient across this region and characterization of the flow pattern. Phasic flow with velocities that return to the baseline suggests that there is not significant obstruction

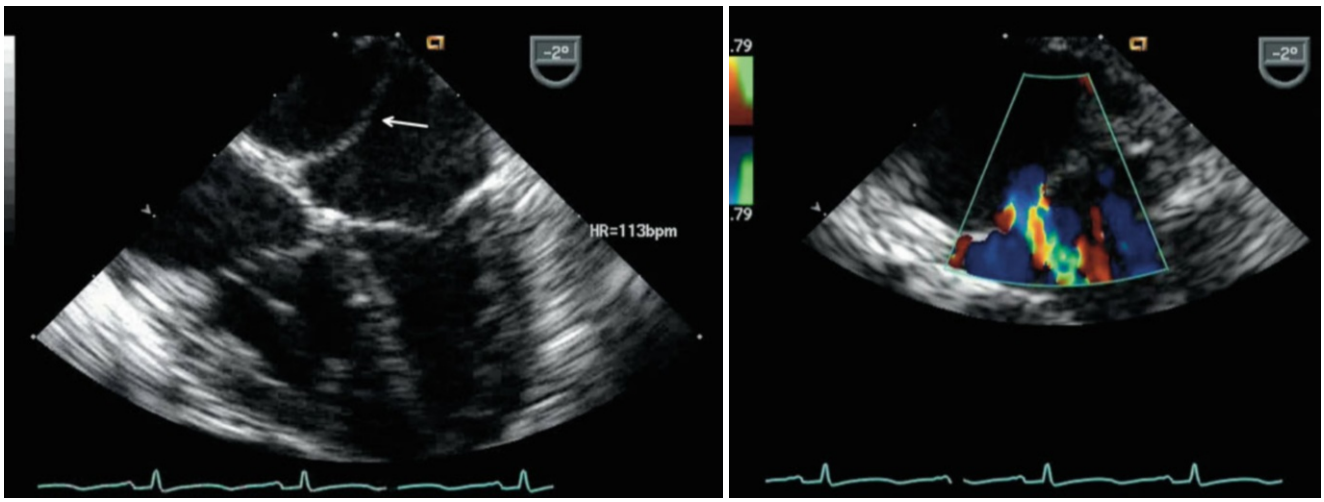

Fig. 7.43 In contrast to the images shown in Fig. 7.42, the cor triatriatum membrane (*arrow*) in this patient was of an obstructive nature. Note the division of the left atrium by the membrane into proximal and distal portions. Color Doppler displays aliased flow across the small central orifice that serves for the egress of blood across the membrane

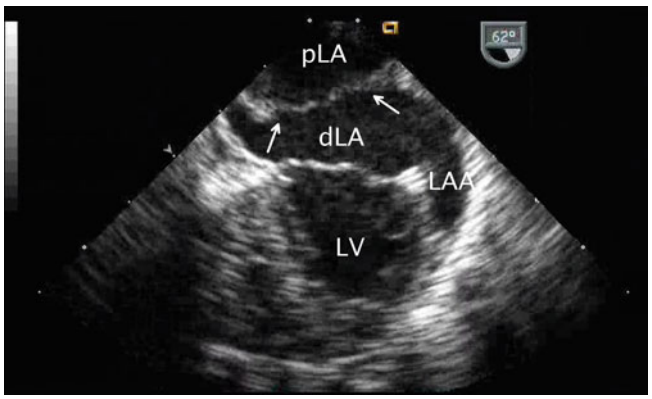

Fig. 7.44 In this mid esophageal view it is seen that the left atrial appendage (*LAA*) lies below the level of the membrane (*arrows*) in cor triatriatum. This is in contrast to a supravalvar mitral ring where the appendage lies above the membrane. *dLA* distal left atrium, *pLA* proximal left atrium, *dLA* distal left atrium, *LV* left ventricle

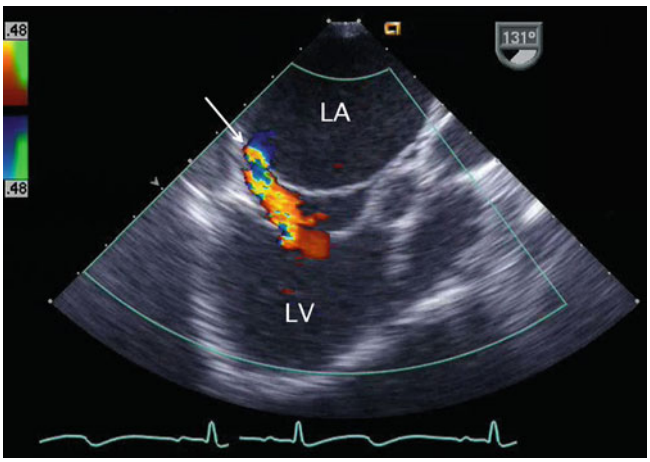

Fig. 7.45 Mid esophageal long-axis view demonstrates a cor triatriatum membrane with a small eccentric posteriorly located orifice. Note the aliased color flow (*arrow*) consistent with obstruction across this area. *LA* left atrium, *LV* left ventricle

Cor triatriatum is associated with other cardiac defects in up to 50 % of cases, most commonly secundum ASD, patent ductus arteriosus, left superior vena cava, and ventricular septal defect. Rare reported associations include tricuspid atresia, Ebstein anomaly of the tricuspid valve, tetralogy of Fallot, atrioventricular septal defect, Shone syndrome and coarctation of the aorta, sinus venosus ASD, and partial/total anomalous pulmonary venous return. Atrial septal communications, when present, typically but not invariably open into the distal (atrial) chamber [68–79].

Cor triatriatum is generally felt to be the result of inadequate incorporation of the common pulmonary vein into the LA during the fifth week of embryologic development. In the usual form, the LA is divided into proximal and distal chambers by a fibromuscular membrane usually with a single (less commonly multiple) restrictive orifice. The location of the LAA with respect to the obstructing membrane is the key anatomic feature that differentiates cor triatriatum from supravalvar mitral ring/stenosis. In cor triatriatum, the LAA is invariably found distal to the membrane in the same chamber with the mitral annulus (atrial chamber). The pulmonary veins drain into the proximal chamber, thus creating a form of pulmonary venous obstruction, which is often moderate to severe and accounts for the typical early clinical presentation of this lesion. However, if the connection between the proximal and distal chambers is not very restrictive, or if an ASD communicating with the pulmonary venous chamber is

Table 7.3 Cor triatriatum (sinister)

Summary of important considerations for TEE assessment
Anatomy of cor triatriatum membrane
Relationship of membrane to left atrial appendage
Exclude partial cor triatriatum
Degree of pulmonary venous obstruction by the cor triatriatum membrane
Anatomy of pulmonary venous return
Assessment of pulmonary hypertension
Presence/absence of atrial septal defect or patent foramen ovale
Determination of which left atrial chamber an existing atrial septal defect/patent foramen ovale communicates with
Evaluation of other associated congenital cardiac lesions
Right heart: tricuspid atresia, Ebstein anomaly, tetralogy of Fallot
Left heart: Shone syndrome, coarctation of the aorta
Miscellaneous: ventricular septal defect, patent ductus arteriosus, sinus venosus atrial septal defect
Ventricular chamber size and systolic function

present allowing a "pop-off" for pulmonary venous return, the hemodynamics may be less significantly affected and the diagnosis may be masked [80, 81]. Partial forms of cor triatriatum also occur, with only the right or left pulmonary veins draining into the proximal chamber.

In cor triatriatum dexter, as indicated, a membrane divides the RA. This is considered the result of a persistent right valve of the sinus venosus. The RA is partitioned (to a greater or lesser degree) into a proximal chamber that includes superior/inferior vena caval return, coronary sinus drainage and atrial septum, and a distal chamber that includes the RAA and tricuspid valve. Patients with cor triatriatum dexter are usually asymptomatic and this is most often reported as an incidental finding, however cases with associated ASDs, hypoplastic right sided structures, Ebstein anomaly, and coronary venous anomalies have been documented [82–84]. If the membrane is sufficiently obstructive, these patients can be cyanotic due to preferential streaming of systemic venous (deoxygenated) blood through an ASD and into the LA.

TTE can generally demonstrate the salient features of cor triatriatum, however TEE may provide optimal views and is useful in assessing the surgical repair [85].

Transesophageal Echocardiographic Evaluation

Anatomic evaluation of cor triatriatum involving the LA begins at the ME 4 Ch view (Fig. 7.42, Video 7.42). Slight retroflexion of the imaging probe maintaining adequate contact optimizes this view and may help prevent compression of the potentially hypertensive pulmonary venous chamber by the probe. Slight counterclockwise turning of the probe and/or rotation of the imaging plane optimally visualizes the LA and demonstrates the obstructing membrane crossing the atrium proximal to the orifice of the LAA. Probe advancement and withdrawal allows scanning of the entire membrane from inferior to superior in this plane. Color Doppler interrogation of a cor triatriatum membrane from the ME 4 Ch and 2 Ch views will most clearly identify the orifice(s) draining to the distal chamber, usually appearing as high velocity, turbulent flow with a lack of phasic variation in the presence of obstruction (Fig. 7.43, Video 7.43).

The connection of the left pulmonary veins proximal to the membrane can be demonstrated from this view (may require further counterclockwise turning and slight advancement or withdrawal of the probe to identify the upper and lower veins). The initial assessment of the left ventricular inflow also begins from this view. Completion of the anatomic evaluation of the LA, cor triatriatum membrane, LAA, and mitral valve/left ventricular inflow (including exclusion of a supravalve mitral ring and/or an abnormal subvalvar mitral apparatus) should be performed via progressive forward axial rotation of the multiplane angle through the following views: mid esophageal mitral commissural (ME Mitral, angle ~60°–70°), ME 2 Ch, and ME LAX (angle 100°–130°) views. Slight counterclockwise probe turning may be necessary. Through this sweep, the LAA will be seen primarily in long axis and the left atrial membrane will be seen attaching to the lateral atrial wall just above the appendage and below the left pulmonary veins (Fig. 7.44, Video 7.44).

Returning to the ME 4 Ch view, clockwise turning of the probe visualizes the mid portion of the interatrial septum to allow for evaluation of associated secundum ASD and/or PFO. Axial rotation of the multiplane angle to the ME Bicaval view, which provides further evaluation of the interatrial septum and systemic venous return, may be performed either at this point or later in the study, if desired. Specific determination of which left atrial chamber (venous or atrial) an interatrial communication enters should be sought in all cases.

In cases with eccentric orifices (Fig. 7.45, Video 7.45), interrogation in multiple planes is essential with forward/backward axial rotation and probe turning as needed to obtain a more ideal Doppler angle of interrogation. TEE windows for Doppler assessment of the membrane in these cases may include the ME Bicaval, ME LAX, ME Mitral, and the DTG views. Spectral Doppler interrogation of the jet across the orifice can be used to estimate the pressure gradient across the membrane to assist in characterizing the severity of pulmonary venous obstruction. Additional information to be obtained from a combination of views includes left ventricular inflow Doppler interrogation (mitral stenosis, regurgitation) and left ventricular diastolic assessment.

Color and pulsed Doppler evaluation of the interatrial septum to assess for associated secundum ASD and/or PFO

should be performed as previously described. Spectral Doppler determination of the peak and mean velocity of left-to-right flow across an ASD communicating with the proximal (venous) chamber can be used to estimate pressure in that chamber. The degree of tricuspid regurgitation should be assessed as well as determination of the Doppler peak velocity of tricuspid regurgitation in order to estimate right ventricular and pulmonary artery systolic pressures. Pulmonary artery diastolic pressure should also be estimated as described in prior sections of this chapter.

Identification of the course and connection of the pulmonary veins may be facilitated by the use of color and spectral Doppler from the ME 4 Ch view with clockwise probe turning for right, and counterclockwise turning for left veins respectively. Color Doppler may also demonstrate the pulmonary veins from the ME Bicaval view, with turning of the probe shaft as described above.

Right ventricular size, wall thickness, and qualitative systolic function, in addition to right atrial size and interventricular septal configuration, may reflect the degree of pulmonary hypertension present and should be evaluated. Pertinent transesophageal and gastric windows include: ME 4 Ch, ME RV In-Out, TG RV In, TG Basal SAX, and TG Mid SAX views. Qualitative assessment of left ventricular systolic function and color/spectral Doppler evaluation of additional associated lesions, as appropriate, is indicated.

Anatomic evaluation of cor triatriatum dexter is similarly performed with a focus on TEE imaging of the systemic venous return, RA, and atrial septum from the LE Situs SAX and lower esophageal inferior vena cava long axis (LE IVC LAX), ME 4 Ch, ME RV In-Out, ME Bicaval, and TG RV In views.

Relevant aspects of the echocardiographic evaluation of this defect are summarized in Table 7.3.

Surgical Considerations

Preoperative Assessment

Important considerations in the preoperative assessment of cor triatriatum involve the following evaluations, as described above: (1) complete left heart examination including attempts to confirm pulmonary venous return (exclude partial anomalous pulmonary venous connections or partial cor triatriatum), (2) 2D imaging of the left atrial membrane, (3) Doppler evaluation of the degree of obstruction across the membrane and estimation of pulmonary venous chamber pressure, (4) exclusion of additional left heart obstructive lesions (supravalve mitral ring, mitral stenosis, left ventricular outflow tract and aortic valve abnormalities/stenosis), (5) Doppler determination of the degree of mitral regurgitation, and (6) evaluation of left ventricular size and qualitative systolic function. Appropriate preoperative evaluation of the right heart includes: (1) right atrial and right ventricular sizes and qualitative right ventricular systolic function, (2) assessment of tricuspid regurgitation severity, and (3) estimation of right ventricular systolic pressure. Presence and anatomic details of any ASD(s) must be determined. Additional associated cardiac structural lesions should be sought out and evaluated as well.

Postoperative Assessment

Surgical intervention for this anomaly typically involves resection of the membrane. Postoperative evaluation includes confirmation of adequate cardiac de-airing and evaluation of the adequacy of the repair. This involves: (1) exclusion of a residual membrane and left atrial obstruction, (2) evaluation of the atrial septum for shunting, because resection of the membrane might be performed through a right atriotomy and an incision in the atrial septum, (3) re-evaluation of tricuspid regurgitation severity and estimation of right ventricular systolic pressure, and (4) qualitative assessment of biventricular systolic function. If other procedures were performed for associated lesions, the adequacy of the surgical intervention for these procedures should be assessed as well.

Summary

TEE contributes to the diagnostic evaluation of interatrial communications and plays an important role in the management of patients affected by these defects in both the operating room and cardiac catheterization settings. Likewise, the transesophageal imaging approach facilitates the characterization of atrial variants and pathologies affecting atrial structures. Further advancements in imaging technologies are likely to further expand the benefits and applications of TEE in the assessment of these structures and corresponding anomalies.

References

1. Seward JB, Khandheria BK, Edwards WD, et al. Biplanar transesophageal echocardiography: anatomic correlations, image orientation, and clinical applications. Mayo Clin Proc. 1990;65:1193–213.
2. Tardif JC, Schwartz SL, Vannan MA, et al. Clinical usefulness of multiplane transesophageal echocardiography: comparison to biplanar imaging. Am Heart J. 1994;128:156–66.
3. Kronzon I, Tunick PA, Freedberg RS, et al. Transesophageal echocardiography is superior to transthoracic echocardiography in the diagnosis of sinus venosus atrial septal defect. J Am Coll Cardiol. 1991;17:537–42.
4. Lin SL, Ting CT, Hsu TL, et al. Transesophageal echocardiographic detection of atrial septal defect in adults. Am J Cardiol. 1992;69:280–2.
5. Hamdan R, Mirochnik N, Celermajer D, et al. Cor Triatriatum Sinister diagnosed in adult life with three dimensional transesophageal echocardiography. BMC Cardiovasc Disord. 2010;10:54.

6. Saric M, Perk G, Purgess JR, et al. Imaging atrial septal defects by real-time three-dimensional transesophageal echocardiography: step-by-step approach. J Am Soc Echocardiogr. 2010;23:1128–35.
7. Faletra FF, Nucifora G, Ho SY. Imaging the atrial septum using real-time three-dimensional transesophageal echocardiography: technical tips, normal anatomy, and its role in transseptal puncture. J Am Soc Echocardiogr. 2011;24:593–9.
8. Johri AM, Witzke C, Solis J, et al. Real-time three-dimensional transesophageal echocardiography in patients with secundum atrial septal defects: outcomes following transcatheter closure. J Am Soc Echocardiogr. 2011;24:431–7.
9. Perez L, Razzouk A, Bansal RC. Real time three-dimensional transesophageal echocardiographic evaluation of a sinus venosus atrial septal defect. Echocardiography. 2011;28:E82–4.
10. Roberson DA, Cui W, Patel D, et al. Three-dimensional transesophageal echocardiography of atrial septal defect: a qualitative and quantitative anatomic study. J Am Soc Echocardiogr. 2011; 24:600–10.
11. Feldt RH, Avasthey P, Yoshimasu F, et al. Incidence of congenital heart disease in children born to residents of Olmsted County, Minnesota, 1950–1969. Mayo Clin Proc. 1971;46:794–9.
12. Anderson RH, Brown NA, Webb S. Development and structure of the atrial septum. Heart. 2002;88:104–10.
13. Ferreira SM, Ho SY, Anderson RH. Morphological study of defects of the atrial septum within the oval fossa: implications for transcatheter closure of left-to-right shunt. Br Heart J. 1992;67:316–20.
14. Brassard M, Fouron JC, van Doesburg NH, et al. Outcome of children with atrial septal defect considered too small for surgical closure. Am J Cardiol. 1999;83:1552–5.
15. Riggs T, Sharp SE, Batton D, et al. Spontaneous closure of atrial septal defects in premature vs. full-term neonates. Pediatr Cardiol. 2000;21:129–34.
16. McMahon CJ, Feltes TF, Fraley JK, et al. Natural history of growth of secundum atrial septal defects and implications for transcatheter closure. Heart. 2002;87:256–9.
17. Basson CT, Cowley GS, Solomon SD, et al. The clinical and genetic spectrum of the Holt-Oram syndrome (heart-hand syndrome). N Engl J Med. 1994;330:885–91.
18. Basson CT, Bachinsky DR, Lin RC, et al. Mutations in human TBX5 [corrected] cause limb and cardiac malformation in Holt-Oram syndrome. Nat Genet. 1997;15:30–5.
19. Schott JJ, Benson DW, Basson CT, et al. Congenital heart disease caused by mutations in the transcription factor NKX2–5. Science. 1998;281:108–11.
20. Vaughan CJ, Basson CT. Molecular determinants of atrial and ventricular septal defects and patent ductus arteriosus. Am J Med Genet. 2000;97:304–9.
21. Garg V, Kathiriya IS, Barnes R, et al. GATA4 mutations cause human congenital heart defects and reveal an interaction with TBX5. Nature. 2003;424:443–7.
22. Ching YH, Ghosh TK, Cross SJ, et al. Mutation in myosin heavy chain 6 causes atrial septal defect. Nat Genet. 2005;37:423–8.
23. Van Praagh S, Carrera ME, Sanders SP, et al. Sinus venosus defects: unroofing of the right pulmonary veins—anatomic and echocardiographic findings and surgical treatment. Am Heart J. 1994;128: 365–79.
24. Jean D, Girard F, Couture P, et al. Transesophageal echocardiographic diagnosis of sinus venosus-type atrial septal defect associated with partial anomalous venous connections during cardiac surgery in adults. J Cardiothorac Vasc Anesth. 1995;9:438–41.
25. Davia JE, Cheitlin MD, Bedynek JL. Sinus venosus atrial septal defect: analysis of fifty cases. Am Heart J. 1973;85:177–85.
26. al Zaghal AM, Li J, Anderson RH, et al. Anatomical criteria for the diagnosis of sinus venosus defects. Heart. 1997;78:298–304.
27. Li J, Al Zaghal AM, Anderson RH. The nature of the superior sinus venosus defect. Clin Anat. 1998;11:349–52.
28. Van Praagh S, Geva T, Lock JE, et al. Biatrial or left atrial drainage of the right superior vena cava: anatomic, morphogenetic, and surgical considerations—report of three new cases and literature review. Pediatr Cardiol. 2003;24:350–63.
29. Sunaga Y, Hayashi K, Okubo N, et al. Transesophageal echocardiographic diagnosis of coronary sinus type atrial septal defect. Am Heart J. 1992;124:1657–9.
30. Quaegebeur J, Kirklin JW, Pacifico AD, et al. Surgical experience with unroofed coronary sinus. Ann Thorac Surg. 1979;27:418–25.
31. Freedom RM, Culham JA, Rowe RD. Left atrial to coronary sinus fenestration (partially unroofed coronary sinus). Morphological and angiocardiographic observations. Br Heart J. 1981;46:63–8.
32. Franz C, Mennicken U, Dalichau H, et al. Abnormal communication between the left atrium and the coronary sinus. Presentation of 2 cases and review of the literature. Thorac Cardiovasc Surg. 1985;33:113–7.
33. Schneider B, Zienkiewicz T, Jansen V, et al. Diagnosis of patent foramen ovale by transesophageal echocardiography and correlation with autopsy findings. Am J Cardiol. 1996;77:1202–9.
34. Waggoner AD, Davila-Roman VG, Hopkins WE, et al. Comparison of color flow imaging and peripheral venous saline contrast during transesophageal echocardiography to evaluate right-to-left shunt at the atrial level. Echocardiography. 1993;10:59–66.
35. Belkin RN, Pollack BD, Ruggiero ML, et al. Comparison of transesophageal and transthoracic echocardiography with contrast and color flow Doppler in the detection of patent foramen ovale. Am Heart J. 1994;128:520–5.
36. Hagen PT, Scholz DG, Edwards WD. Incidence and size of patent foramen ovale during the first 10 decades of life: an autopsy study of 965 normal hearts. Mayo Clin Proc. 1984;59:17–20.
37. Fisher DC, Fisher EA, Budd JH, et al. The incidence of patent foramen ovale in 1,000 consecutive patients. A contrast transesophageal echocardiography study. Chest. 1995;107:1504–9.
38. Agnetti A, Carano N, Sani E, et al. Cryptogenic stroke in children: possible role of patent foramen ovale. Neuropediatrics. 2006;37:53–6.
39. Bartz PJ, Cetta F, Cabalka AK, et al. Paradoxical emboli in children and young adults: role of atrial septal defect and patent foramen ovale device closure. Mayo Clin Proc. 2006;81:615–8.
40. Meissner I, Khandheria BK, Heit JA, et al. Patent foramen ovale: innocent or guilty? Evidence from a prospective population-based study. J Am Coll Cardiol. 2006;47:440–5.
41. Hausmann D, Daniel WG, Mugge A, et al. Value of transesophageal color Doppler echocardiography for detection of different types of atrial septal defect in adults. J Am Soc Echocardiogr. 1992; 5:481–8.
42. Oh JK, Seward JB, Khandheria BK, et al. Visualization of sinus venosus atrial septal defect by transesophageal echocardiography. J Am Soc Echocardiogr. 1988;1:275–7.
43. Watanabe F, Takenaka K, Suzuki J, et al. Visualization of sinus venosus-type atrial septal defect by biplane transesophageal echocardiography. J Am Soc Echocardiogr. 1994;7:179–81.
44. Pascoe RD, Oh JK, Warnes CA, et al. Diagnosis of sinus venosus atrial septal defect with transesophageal echocardiography. Circulation. 1996;94:1049–55.
45. Hellenbrand WE, Fahey JT, McGowan FX, et al. Transesophageal echocardiographic guidance of transcatheter closure of atrial septal defect. Am J Cardiol. 1990;66:207–13.
46. Ishii M, Kato H, Inoue O, et al. Biplane transesophageal echo-Doppler studies of atrial septal defects: quantitative evaluation and monitoring for transcatheter closure. Am Heart J. 1993;125:1363–8.
47. Hijazi ZM, Cao Q, Patel HT, et al. Transesophageal echocardiographic results of catheter closure of atrial septal defect in children and adults using the Amplatzer device. Am J Cardiol. 2000;85:1387–90.
48. Latiff HA, Samion H, Kandhavel G, et al. The value of transesophageal echocardiography in transcatheter closure of atrial septal defects in the oval fossa using the Amplatzer septal occluder. Cardiol Young. 2001;11:201–4.

49. Figueroa MI, Balaguru D, McClure C, et al. Experience with use of multiplane transesophageal echocardiography to guide closure of atrial septal defects using the Amplatzer device. Pediatr Cardiol. 2002;23:430–6.
50. Kleinman CS. Echocardiographic guidance of catheter-based treatments of atrial septal defect: transesophageal echocardiography remains the gold standard. Pediatr Cardiol. 2005;26:128–34.
51. Stevenson JG. Role of intraoperative transesophageal echocardiography during repair of congenital cardiac defects. Acta Paediatr Suppl. 1995;410:23–33.
52. Rosenfeld HM, Gentles TL, Wernovsky G, et al. Utility of intraoperative transesophageal echocardiography in the assessment of residual cardiac defects. Pediatr Cardiol. 1998;19:346–51.
53. Tempe DK, Sharma S, Banerjee A, et al. The utility of transesophageal echocardiography for detecting residual shunt in a patient undergoing atrial septal defect repair. Anesth Analg. 2007;104: 777–8.
54. Dixon AS. Juxtaposition of the atrial appendages; two cases of an unusual congenital cardiac deformity. Br Heart J. 1954;16:153–64.
55. Frescura C, Thiene G. Juxtaposition of the atrial appendages. Cardiovasc Pathol. 2012;21(3):169–79.
56. Van Praagh S, O'Sullivan J, Brili S, et al. Juxtaposition of the morphologically left atrial appendage in solitus and inversus atria: a study of 18 postmortem cases. Am Heart J. 1996;132: 391–402.
57. Van Praagh S, O'Sullivan J, Brili S, et al. Juxtaposition of the morphologically right atrial appendage in solitus and inversus atria: a study of 35 postmortem cases. Am Heart J. 1996;132:382–90.
58. Lai WW, Ravishankar C, Gross RP, et al. Juxtaposition of the atrial appendages: a clinical series of 22 patients. Pediatr Cardiol. 2001;22:121–7.
59. Anjos RT, Ho SY, Anderson RH. Surgical implications of juxtaposition of the atrial appendages. A review of forty-nine autopsied hearts. J Thorac Cardiovasc Surg. 1990;99:897–904.
60. Stumper O, Rijlaarsdam M, Vargas-Barron J, et al. The assessment of juxtaposed atrial appendages by transoesophageal echocardiography. Int J Cardiol. 1990;29:365–71.
61. Zhang YQ, Yu ZQ, Zhong SW, et al. Echocardiographic assessment of juxtaposition of the right atrial appendage in children with congenital heart disease. Echocardiography. 2010;27:878–84.
62. Tyrrell MJ, Moes CA. Congenital levoposition of the right atrial appendage. Its relevance to balloon septostomy. Am J Dis Child. 1971;121:508–10.
63. Rice MJ, Seward JB, Hagler DJ, et al. Left juxtaposed atrial appendages: diagnostic two-dimensional echocardiographic features. J Am Coll Cardiol. 1983;1:1330–6.
64. Lee ML, Wu MH, Wang JK, et al. Echocardiographic features of left juxtaposed atrial appendages associated with dextrotransposition of the great arteries. Pediatr Cardiol. 1996;17:63–6.
65. Chin AJ, Bierman FZ, Williams RG, et al. 2-dimensional echocardiographic appearance of complete left-sided juxtaposition of the atrial appendages. Am J Cardiol. 1983;52:346–8.
66. Tuccillo B, Stumper O, Hess J, et al. Transoesophageal echocardiographic evaluation of atrial morphology in children with congenital heart disease. Eur Heart J. 1992;13:223–31.
67. Viswanathan S, Vaidyanathan B, Kumar RK. Thrombus in a juxtaposed right atrial appendage. Cardiol Young. 2007;17:574.
68. Van Praagh R, Corsini I. Cor triatriatum: pathologic anatomy and a consideration of morphogenesis based on 13 postmortem cases and a study of normal development of the pulmonary vein and atrial septum in 83 human embryos. Am Heart J. 1969;78:379–405.
69. Marin-Garcia J, Tandon R, Lucas RVJ, et al. Cor triatriatum: study of 20 cases. Am J Cardiol. 1975;35:59–66.
70. Roper PC, Wright JS, McCredie RM, et al. Cor triatriatum associated with unilateral anomalous pulmonary venous drainage in an infant. Aust Paediatr J. 1981;17:122–4.
71. Hess J, Brenken U, Eygelaar A, et al. Successful management of cor triatriatum associated with anomalous pulmonary/systemic venous connection in an infant. Pediatr Cardiol. 1982;2:319–22.
72. Ostman-Smith I, Silverman NH, Oldershaw P, et al. Cor triatriatum sinistrum. Diagnostic features on cross sectional echocardiography. Br Heart J. 1984;51:211–9.
73. Grifka RG, Vincent JA. Abnormalities of the left atrium and mitral valve, including mitral valve prolapse. In: Garson AT, Bricker JT, Fisher DJ, et al., editors. The science and practice of pediatric cardiology. 2nd ed. Baltimore: Williams and Wilkins; 1998.
74. Binotto MA, Aiello VD, Ebaid M. Coexistence of divided left atrium (cor triatriatum) and tetralogy of Fallot. Int J Cardiol. 1991;31:97–9.
75. Kerensky RA, Bertolet BD, Epstein M. Late discovery of cor triatriatum as a result of unilateral pulmonary venous obstruction. Am Heart J. 1995;130:624–7.
76. Eidem BW, Cetta F. Unusual finding of cor triatriatum in a newborn with hypoplastic left heart syndrome. J Am Soc Echocardiogr. 2001;14:850–2.
77. Ito M, Kikuchi S, Hachiro Y, et al. Congenital pulmonary vein stenosis associated with cor triatriatum. Ann Thorac Surg. 2001;71: 722–3.
78. Hiramatsu T, Komori S, Okamura Y, et al. Surgical case of partial anomalous pulmonary venous connection to superior vena cava with cor triatriatum: Williams' modification and excision of diaphragm. Heart Vessels. 2008;23:433–5.
79. Tachibana K, Takagi N, Osawa H, et al. Cor triatriatum and total anomalous pulmonary venous connection to the coronary sinus. J Thorac Cardiovasc Surg. 2007;134:1067–9.
80. Jacobstein MD, Hirschfeld SS. Concealed left atrial membrane: pitfalls in the diagnosis of cor triatriatum and supravalve mitral ring. Am J Cardiol. 1982;49:780–6.
81. Krasemann Z, Scheld HH, Tjan TD, et al. Cor triatriatum: short review of the literature upon ten new cases. Herz. 2007; 32:506–10.
82. Fiorilli R, Argento G, Tomasco B, et al. Cor triatriatum dexter diagnosed by transesophageal echocardiography. J Clin Ultrasound. 1995;23:502–4.
83. Inoue Y, Tomomasa T, Okada Y, et al. Divided right atrium associated with extensive coronary vein abnormalities. Pediatr Cardiol. 2002;23:68–70.
84. Eroglu ST, Yildirir A, Simsek V, et al. Cor triatriatum dexter, atrial septal defect, and Ebstein's anomaly in an adult given a diagnosis by transthoracic and transesophageal echocardiography: a case report. J Am Soc Echocardiogr. 2004;17:780–2.
85. Shuler CO, Fyfe DA, Sade R, et al. Transesophageal echocardiographic evaluation of cor triatriatum in children. Am Heart J. 1995;129:507–10.